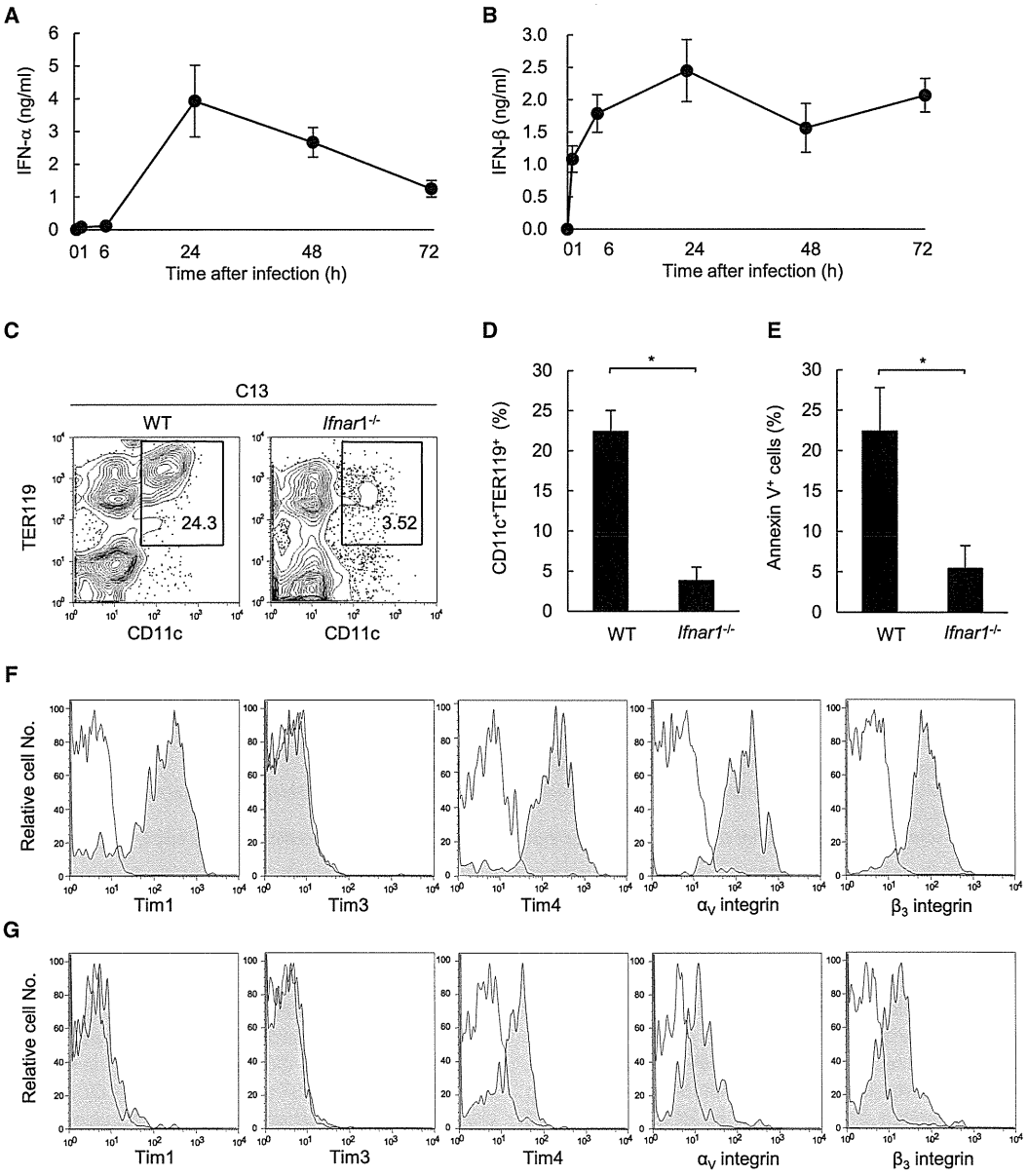

Figure 4. Essential Role of Type I IFNs in C13-Induced Hemophagocytosis

(A and B) Kinetics of serum IFN-α (A) and IFN-β (B) production in WT mice after 2 × 10^6 pfu C13 infection.

(C) Representative flow cytometry (FCM) profiles of $CD11c^+TER119^+$ cells in the peripheral blood of WT and *Ifnar1*$^{-/-}$ mice 24 hr after 2 × 10^6 pfu C13 infection.

(D and E) The percentage of $CD11c^+TER119^+$ cells (D) and annexin V^+ cells among $TER119^+$ cells (E) in the peripheral blood of WT mice 4 hr and 24 hr after injection of 2 × 10^6 pfu C13, respectively.

(F and G) Expression of "eat me" signal receptors on $CD11c^+TER119^+$ cells in the peripheral blood of WT (F) and *Ifnar1*$^{-/-}$ (G) mice 24 hr after 2 × 10^6 pfu C13 infection. Shaded histograms represent cells stained with mAbs specific for the indicated molecules, and open histograms show labeling with isotype controls. Data represent the mean ± SD of three independent experiments. *$p < 0.01$. See also Figure S4.

were obtained from the coculture in which Mo-DCs and granulocytes, the other apoptotic population in C13-infected mice (Figures S4D and S4E), were used in the same experiment (Figure S6A). Notably, the amounts of IL-10 secreted from the Mo-DCs that engulfed erythroid cells were 60 pg/ml and, from those that engulfed granulocytes, were 40 pg/ml in the same experiment (Figure 6E; Figure S6A). These results suggested that granulocytes are slightly less potent on a per-cell basis than erythroid cells for inducing IL-10 secretion from Mo-DCs. To definitively show the contribution of these integrins to the IL-10 secretion from Mo-DCs, we performed ex vivo hemophagocytosis assay, in which Mo-DCs and erythroid cells, sorted

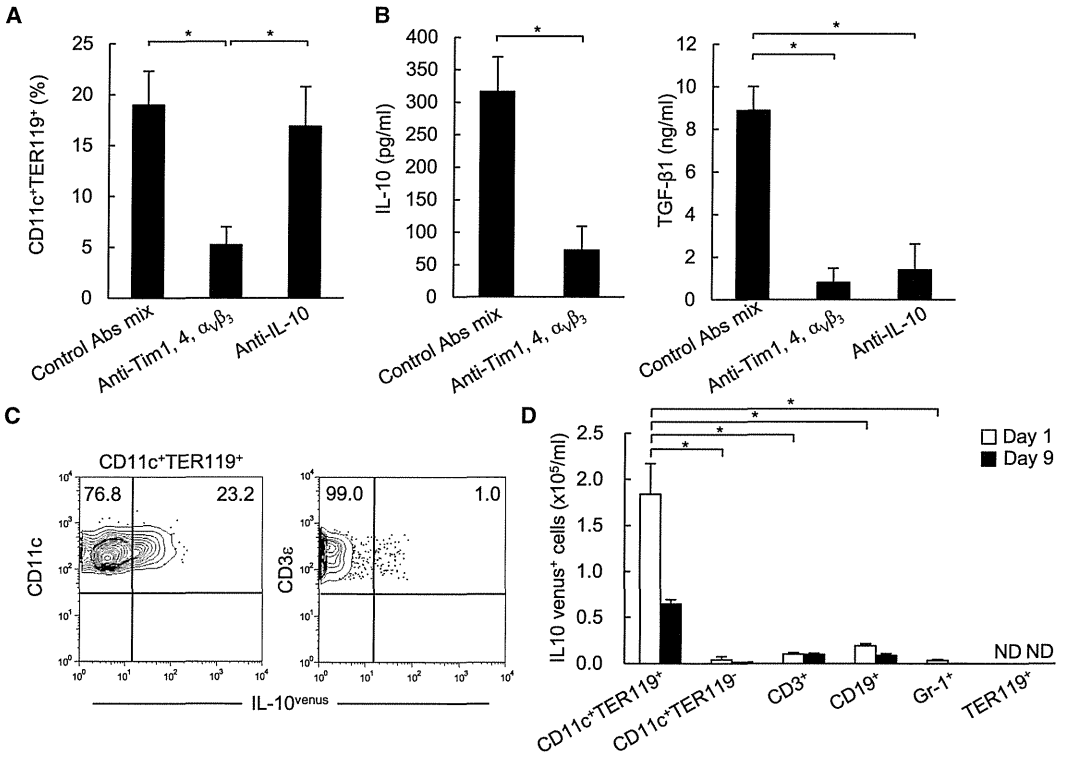

Figure 5. Hemophagocytosis-Dependent IL-10 Production from MO-DCs upon C13 Infection

(A) C13-induced hemophagocytosis in the peripheral blood of WT mice treated with either isotype control Ab cocktails (500 μg each), blocking antibodies against PS receptors, or IL-10 (500 μg each).

(B) IL-10 and TGF-β1 serum amounts 24 hr after C13 infection with the injection of isotype control Ab cocktails (500 μg each), Abs to block PS receptors or neutralize IL-10.

(C) A representative FCM profile of IL-10 Venus expression in the indicated cell populations from the peripheral blood of *Il10*^{Venus} reporter mice 24 hr after C13 infection.

(D) The absolute number of cells expressing IL-10 Venus in the indicated cell populations from the peripheral blood of *Il10*^{Venus} reporter and WT mice 1 and 9 days after C13 infection. Data represent the mean ± SD from three independent experiments. *p < 0.01. See also Figure S5.

separately from the BM of WT and *Mfge8*$^{-/-}$ mice after C13 infection, were cocultured in all combinations (Figure 6F). Importantly, the IL-10 secretion was selectively impaired when *Mfge8*$^{-/-}$Mo-DCs were used for the coculture, demonstrating that the IL-10 secretion from Mo-DCs is MFG-E8-mediated and thus dependent on both integrin $\alpha_v\beta_3$ and $\alpha_v\beta_5$ (Figure 6F).

We also examined the apoptotic status of these cells during later time points; i.e., 8, 16, and 24 days after the infection. The numbers of apoptotic erythroid cells were much reduced and comparable to those of granulocytes (Figure S6B), and the numbers of IL-10 producing cells were substantially lower, compared with that at an early phase of infection (Figure S6C). As observed at an early phase of infection, lymphocyte populations, i.e., T and B cells, hardly became apoptotic during later time points (Figure S6B). These results implied that erythroid cells and granulocytes equally contribute to phagocytosis-mediated IL-10 production during later phase of infection.

Hemophagocytosis Prevents Immune-Responses-Mediated Damage and Ensure the Host's Survival

What is the physiological relevance of the hemophagocyte-derived IL-10 in viral infection? Interestingly, blocking hemophagocytosis with PS receptor Abs or IL-10 activity with IL-10-neutralizing Ab enhanced the virus-specific CTL induction (Figures 7A and 7B), CTL-mediated liver-damage (Zinkernagel et al., 1986) (serum AST and ALT) (Figure 7C), and mortality (Figure 7D). In the context of CTL activity, we also found that blocking hemophagocytosis or IL-10 activity diminished the CTL expression of PD-1 (data not shown), which causes CTL exhaustion in C13 infection (Barber et al., 2006). Because Tim-1- and Tim-4-signaling can alter immune responses in some cases (Xiao et al., 2007, 2011; Rodriguez-Manzanet et al., 2008), we examined whether anti-Tim-1 and anti-Tim-4 Abs could modulate immune responses in C13-infected WT mice. However, injecting anti-Tim-1 and anti-Tim-4 Abs did not alter the frequency of hemophagocytosis in the peripheral blood, IL-10 amounts and C13 virus titers in the sera, and percentage and absolute number of IL-10^{Venus+} CD11c^{+}TER119^{+} cells (data not shown), suggesting that these Abs do not significantly affect virus-specific immune responses in vivo, at least in this experimental setting.

To further confirm the importance of the hemophagocyte-derived IL-10 in fine-tuning excessive immune responses in vivo, we infected *Cd11c-cre Il10*$^{fl/fl}$ mice, in which the

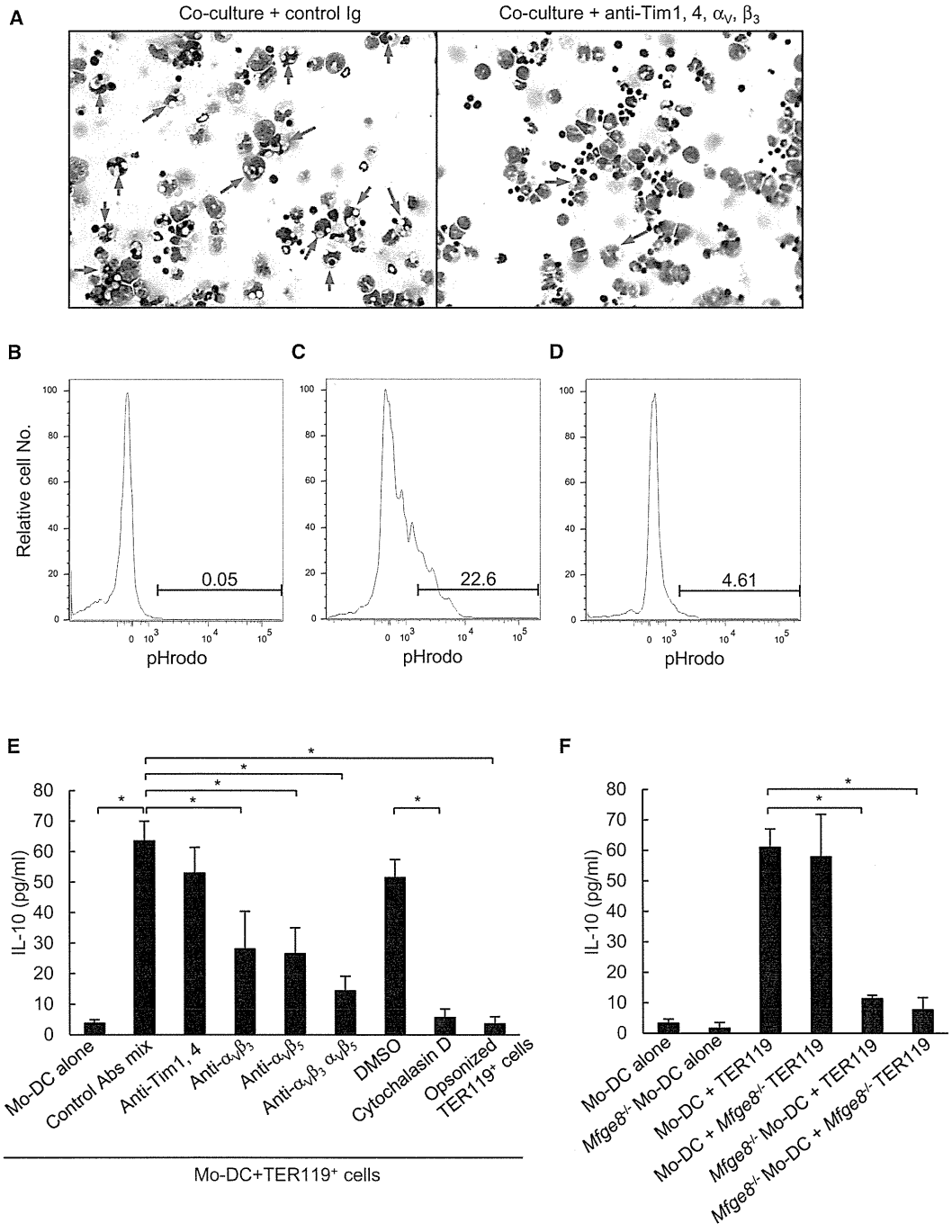

Figure 6. Critical Role of MFG-E8-Integrin Signal in IL-10 Production from Mo-DCs

(A–F) Ex vivo hemophagocytosis assay. TER119$^-$ Mo-DCs and TER119$^+$ erythroid cells were separately sorted from the BM of LCMV C13 infected WT or *Mfge8*$^{-/-}$ mice. The Mo-DCs were pretreated with control rat Ig (A, left panel, and C) or Abs to block PS receptors (B, right panel, and D), and cocultured with pHrodo-labeled TER119$^+$ erythroid cells for 2 hr. The cells were stained with Diff-Quick. Red arrows indicate hemophagocytes. Original magnification, x20 (A). Representative FCM profiles of Mo-DCs cocultured with unlabeled- (B), pHrodo-labeled-erythroid cells (C and D). IL-10 amount in the indicated coculture supernatants is shown (E and F). Data represent the mean ± SD of three independent experiments. *$p < 0.01$. See also Figure S6.

hemophagocytes cannot produce IL-10, with C13. While the numbers of Mo-DCs performing hemophagocytosis in C13-infected *Cd11c-cre Il10*$^{fl/fl}$ mice were comparable to those seen in control WT mice (Figure 7E), the serum IL-10 production was greatly reduced (Figure 7F), confirming that hemophagocytes were the major source of IL-10 in vivo under these infectious

conditions. As with WT mice in which hemophagocytosis was blocked, the *Cd11c-cre Il10*$^{fl/fl}$ mice showed excessive CTL activity, tissue damage, and mortality when infected with C13 (Figure 7G–7J). Taken together, these results point to hemophagocytosis as machinery for preventing excessive immune response-mediated damage, thus assuring the host's survival in the face of severe viral infection.

In summary, our findings indicate that hemophagocytosis induced by C13 infection occurs in sequential steps (Figure S7).

DISCUSSION

We found that hemophagocytosis could be detected by staining with and without permeabilization. In this context, we would like to stress that hemophagocytosis is a sequential event; that is, apoptotic erythroid cells exposing PS are initially attached to PS receptors expressed on the Mo-DCs and are then gradually phagocytosed into the cells. Therefore, even without permeabilization, these cells can be detected as CD11c$^+$TER119$^+$ cells. Supporting the specific recognition of apoptotic erythroid cells by PS receptors on Mo-DCs, hemophagocytosis detected without permeabilization was significantly reduced in WT mice in which hemophagocytosis was blocked with anti-PS receptor Abs or with suramin, a competitive inhibitor of ATP-P2Y2 binding. In C13-infected *Ifnar1*$^{-/-}$ mice, both PS exposure on erythroid cells and PS receptor induction on Mo-DCs were impaired, suggesting that type I IFNs are critically involved in these processes. Because it is well known that CpG injection induces type I IFN production, it is likely that CpG-induced type I IFNs induce apoptosis of erythroid cells. Indeed, ex vivo IFN-α stimulation directly induced apoptosis of erythroid cells. F4/80$^+$ macrophages are reported to be the hemophagocytosis-performing cells in the spleen of mice infused with IFN-γ (Zoller et al., 2011). In this context, we found that the hemophagocytosis-performing Mo-DCs clearly expressed F4/80, suggesting that the previously reported F4/80$^+$ macrophages and the Mo-DCs are presumably overlapping populations (Domínguez and Ardavín, 2010).

The uptake of experimentally (UV-irradiation, staurosporine, etc.) induced apoptotic peripheral blood lymphocytes, neutrophils, and peripheral blood T cells or Jurkat T cells by phagocytes induces IL-10 production, which suppresses proinflammatory cytokine production (Voll et al., 1997; Byrne and Reen, 2002; Kim et al., 2004). However, it remains unknown whether such ex vivo observations are consistent with and represent the in vivo situation under severe inflammatory conditions. Remarkably, we showed that, upon CpG injection or LCMV C13 infection, most of the apoptotic cells were erythroid cells and a small number were granulocytes. As a result, Mo-DCs preferentially engulfed apoptotic erythroid cells, leading to IL-10 production. Given these findings, we do not exclude the contribution of granulocytes, although it is relatively minor, to the IL-10 secretion from Mo-DCs. Consistent with our findings, the type I IFN-dependent apoptosis of erythroid cells, but not of neutrophils or monocytes, is observed in DNase II-deficient mice (Kawane et al., 2001; Yoshida et al., 2005). These results suggested that type I IFN signaling is required for the recruitment of nucleated erythroid cells to the peripheral blood and that, compared with other hematopoietic cells, erythroid cells are relatively sensitive to type I IFN signaling and therefore become apoptotic. Indeed, IFN-α induces apoptosis in human erythroid cells (Tarumi et al., 1995). Notably, these phenotypes observed in DNase II-deficient mice are consistent with those in WT mice injected with CpG or infected with C13.

Although hemophagocytosis is viewed as an indicator of hemophagocytic syndrome and other severe inflammatory conditions (Clark 2007; Lambeth, 2007; Rouse and Sehrawat, 2010), our findings suggest that it rather represents a possible biomarker of anti-inflammatory responses in the host. Very recently, it was reported that repeatedly injecting CpG induces hemophagocytic syndrome-like or macrophage activation syndrome-like disease in mice (Behrens et al., 2011). When IL-10 signaling is blocked in this model, a more severe disease with larger numbers of hemophagocytosis develops, raising two possibilities; first, hemophagocytosis contributes to the severity of the disease, and second, it is induced, as a negative feedback machinery, to suppress severe inflammatory responses. We propose here that hemophagocytosis is a prerequisite for IL-10 production and that IL-10 is secreted by Mo-DCs in a manner dependent on hemophagocytosis, leading to anti-inflammatory effects of IL-10 to fine-tune immune responses. In humans, hemoglobin uptake by CD163$^+$ macrophages induces the expression of the anti-inflammatory heme oxygenase (HO-1) ex vivo (Schaer et al., 2006a), and HO-1 expression is detected in hemophagocytic CD163$^+$ macrophages in the BM of patients with fatal sepsis (Schaer et al., 2006b). Interestingly, CD163 expression is inducible by IL-10, implying that this anti-inflammatory pathway might also contribute to the prevention of immune responses in vivo.

In acute infections, pathogen growth correlates well with indicators of deteriorating health, and inducing immune responses usually restores health by reducing the pathogen load. However, our findings show that, during severe viral infections, immune responses unaccompanied by efficient hemophagocytosis-mediated fine-tuning lead to a further deterioration in health and eventually to severe immune response-mediated self-damage, despite the virus being effectively eradicated. Of interest, aberrant immune activation with impaired IFN-α expression, a possible cause of limited hemophagocytosis, was evident in macaques infected with the 1918 Spanish pandemic virus (Kobasa et al., 2007).

The more severe the infection, the stronger the immune response must be. The stronger the immune response, the greater the regulatory control must be. Given that most viruses that cause hemophagocytosis, including Epstein-Barr virus, cytomegalovirus, and HIV (Larroche and Mouthon, 2004; Janka, 2007; Maakaroun et al., 2010), establish chronic infections in humans (Clerici et al., 1996; Nordøy et al., 2000; Budiani et al., 2002), the induction of hemophagocytosis might allow the virus to persist in the host, ensuring host survival by preventing immune response-mediated damage. Considering this trade-off between host and pathogen, our findings may be valuable not only in extending our understanding of immune biology but also in identifying therapeutic targets for severe inflammatory diseases.

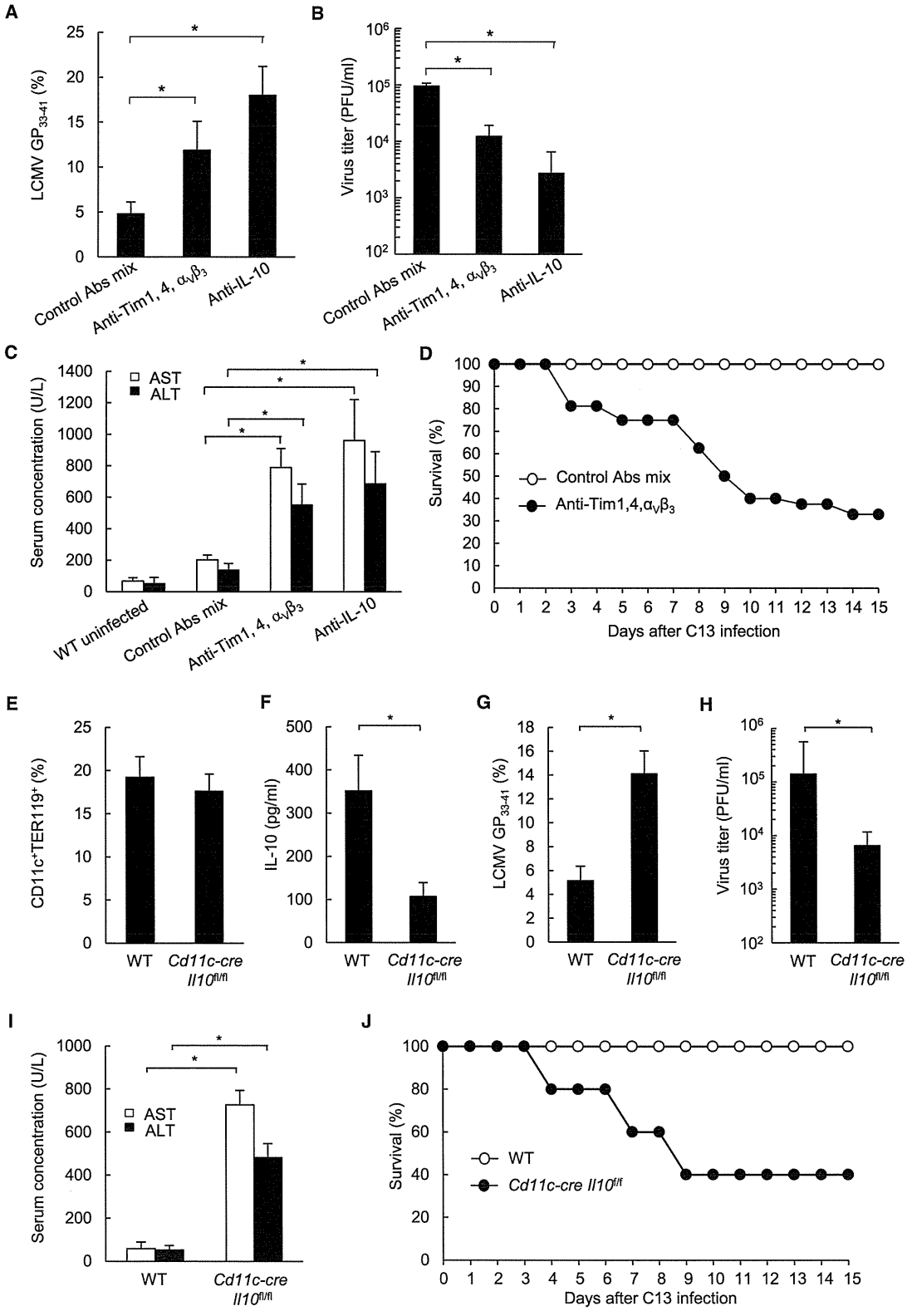

(legend on next page)

EXPERIMENTAL PROCEDURES

Mice

C57BL/6J (B6, Clea), B6.*Cx$_3$cr1*$^{GFP/+}$ (Jackson) (Jung et al., 2000), B6.*Ccr2*$^{-/-}$ (Jackson) (Boring et al., 1997), B6.*Ccl2*$^{-/-}$ (Lu et al., 1998), B6.*Ifnar1*$^{-/-}$ (B&K Universal), B6.*Il-10*^{Venus} (Atarashi et al., 2011), B6.*Cd11c*-Cre (Jackson) (Stranges et al., 2007), B6.*Mfge8*$^{-/-}$ (Hanayama et al., 2004), and B6.*Il10*$^{fl/fl}$ (Roers et al., 2004) mice were maintained in our SPF facility. All animal experiments were approved by the Institutional Animal Care Committees of Akita University and Tokyo Medical and Dental University.

Reagents and In Vivo Injection

LPS, MDP, and cytochalasin D were purchased from Sigma-Aldrich. Other reagents were obtained as follows: poly I:C (GE Healthcare), R848 (Invivogen), CpG (ODN-1668 [5′-TCCATGACGTTCCTGATGCT-3′]; Hokkaido System Science), iE-DAP (Invivogen), and recombinant mouse interferon-α (Dainion Sumitomo Pharma). Mice were intravenously (i.v.) injected with TLR ligands (200 μg poly I:C, 100 μg LPS, 100 μg R848, or 200 μg CpG) or Nod ligands (100 μg iE-DAP or 100 μg MDP). Mice were infected by i.v. injection of viruses (2×10^6 pfu LCMV Armstrong or Clone 13).

Diff-Quick Stain

CD11c$^+$TER119$^+$ cells were sorted from the BM of CpG-injected or LCMV C13-infected mice, cytospun at 500 *g* for 5 min onto a slide glass, and stained with Diff-Quick (Sysmex).

Electron Microscopy

CD11c$^+$TER119$^+$ cells were sorted from the peripheral blood of CpG-injected mice, fixed with 2.5% glutaraldehyde in 0.1 M phosphate buffer pH7.2, washed overnight at 4c°C in the same buffer, and postfixed with 1% OsO_4 at 4°C for 2 hr. Then, the cells were dehydrated in a graded in a series of ethanol and embedded in Epon 812. Ultrathin (1 μm) sections were collected on copper grids and with uranyl acetate and lead citrate and then examined by transmission electron microscope, H-7100 (Hitachi).

Hemophagocytosis Blocking

To block ATP activity, we intraperitoneally (i.p.) injected 6 mg suramin into WT mice 30 min after CpG or poly I:C injection or 3 and 6 days after C13 infection. To block "eat me" signal receptors, we gave WT mice 500 μg rat IgG (control) or 500 μg anti-Tim-1 mAb (RMT1-10) (Nakayama et al., 2009), 500 μg anti-Tim-4 mAb (RMT4-54) (Nakayama et al., 2009), 500 μg anti-α_V mAb (RMV-7) (Takahashi et al., 1990), or 500 μg anti-β_3 mAb (HMβ3-1) (Yasuda et al., 1995), or isotype control Ab cocktails including rat IgG2a, rat IgG2c, and hamster IgG (500 μg of each) by i.v., singly or in combination as indicated, 60 min and 120 min after CpG injection or viral infection. To block cytokines, we injected 500 μg rat IgG (control) or 500 μg anti-IL-10 (JES5-2A5) i.p. into WT mice 1 day and 3 days after C13 infection.

ELISAs

Cytokine and chemokine serum amounts were determined by ELISA kits according to the manufacturer's instructions (CCL2, IL-10, and TGF-β1, R&D; CCL7 and CCL12, Bender Med Systems). ATP, AST, and ALT serum amounts were determined by a luciferin-luciferase assay with an ATP assay kit (Toyo Ink) and a Fuji DRI-CHEM 3500 V analyzer (Fuji Medical Systems), respectively, according to the manufacturer's instructions.

Flow Cytometric Analysis and Cell Sorting

Antibodies against the following molecules were used for flow cytometric analysis and cell sorting: CD3ε (145-2C11), CD11b (M1/70), CD11c (N418), TER119 (TER119), CD19 (MB19-1), CD40 (1C10), CD80 (16-10A1), CD86 (GL19), NK1.1 (PK136), MHC class II (I-A and I-E; M 5/114.15.2), α_V (RMV-7), β_3 (2C9.G3), PD-1 (RMP1-30) (all from eBioscience), F4/80 (BM8) (Biolegend), and Ly6c (AL-219) (BD), Stabilin-2 (#34-2) (MBL), Tryo-3 (109646), Axl (175128), and MerTK (108921) (all from R&D). Antibodies against Tim-1 (RMT1-17), Tim-3 (RMT3-23), and Tim-4 (RMT4-53) were as described previously (Nakayama et al., 2009). To analyze hemophagocytosis, we used two protocols. First, peripheral blood samples were collected into heparin-containing tubes and immediately maintained on ice. Red blood cells were lysed by adding 10 ml ACK buffer to the samples and keeping them on ice for 10 min. After washing with cold PBS, the samples were stained with APC-anti-CD11c, PE-anti-CD11b, and FITC-anti-TER119. This protocol detected apoptotic erythroid cells exposed on Mo-DC surfaces, including cells attached to Mo-DC PS receptors or undergoing phagocytosis. Second, a recently reported protocol was used to detect the intracellular localization of apoptotic erythroid cells (Zoller et al., 2011). In detail, TER119 exposed on MO-DC surfaces was first blocked with saturating amounts of an unlabeled Ab against TER119 (10 μg/10 μl) and then permeabilized with a BD Cytofix/Cytoperm kit (BD) and stained with FITC-anti-TER119 and APC-anti-CD11c Abs. Apoptotic cells were detected with PE-annexin V (BD) according to the manufacturer's instructions. To purify inflammatory monocytes, defined as CX3CR1$^+$Ly6c^{hi}CD11b$^+$CD11c$^-$ cells, we pre-enriched BM CD3ε$^-$CD19$^-$NK1.1$^-$ cells from *Cx$_3$cr1*$^{GFP/+}$ mice by using a PE-Cy5-conjugated antibody mixture (CD3 ε, CD19, NK1.1), Cy5 microbeads, and an AutoMACSpro separation system (Miltenyi Biotec). The cells were then stained with biotin-anti-Ly6c, PE-anti-CD11b, and APC-anti-CD11c antibodies, secondarily labeled with streptavidin-PE-Cy7, sorted on a MoFlo instrument (Beckman Coulter), and analyzed on a FACSCanto II (BD) in conjunction with FlowJo software (TreeStar).

CTL Response and Virus Titer Detection

Splenocytes were harvested 9 days after infection. To detect LCMV-specific CTL, splenocytes were stained with FITC-anti-CD8 (KT15) (MBL), APC-anti-CD3ε, and PE-H-2D^b-LCMV gp_{33-41} tetramer (MBL). IFN-γ induction was analyzed by stimulating splenocytes with an LCMV H-2D^b-binding peptide (gp_{33-41}, KAVYNFATM; Peptide Institute), 50 U/ml murine IL-2, and Golgi Stop (BD) prior to incubation with CD8α antibodies. Cells were then fixed and stained with IFN-γ-PE antibodies in PermWash solution (BD) according to the manufacturer's recommendation. For virus titration, MC57G cells were incubated with 10-fold serial dilutions of LCMV-containing serum in a 24-well plate at 37°C for 48 hr. Cells were then fixed with 4% formalin, permeabilized with 0.5% Triton X, and incubated with 10% fetal bovine serum. After incubation with murine LCMV immunoglobulin G1 (IgG1; Progen Biotechnik) and anti-mouse IgG-horseradish peroxidase (GE Healthcare), the plates were stained with an AEC peroxidase substrate kit (Vector Laboratories) and virus plaques were counted for each well.

Quantitative RT-PCR

Total RNA was extracted with an RNeasy Mini Kit (QIAGEN), and cDNA was synthesized with random hexamers and SuperScript III reverse transcriptase. For real-time PCR, cDNA products equivalent to RNA from 2,000 cells were amplified with a LightCycler®480 and SYBR Green I Master (Roche Diagnostics). The data were normalized to the amounts of *gapdh* RNA expression in each sample. The primers used for real-time PCR were as follows: *Ccr2*, 5′-AT

Figure 7. Physiological Significance of C13 Infection-Induced Hemophagocytosis

(A–C) Percentage of LCMV GP_{33-41}-specific CD8$^+$ T cells in the spleen (A), titer of LCMV C13 in the serum (B), and amount of AST/ALT in the serum (C) of uninfected WT mice and WT mice 9 days after LCMV C13 infection, with or without the injection of Abs to block PS receptors or neutralize IL-10.

(D) Survival (%) of WT mice after LCMV C13 infection with or without the injection of Abs to block PS receptors.

(E–J) Hemophagocytosis (%) (E) and IL-10 amounts (F) in the peripheral blood of WT mice 24 hr after C13 infection. The percentage of LCMV GP_{33-41}-specific CD8$^+$ T cells in the spleen (G), titer of LCMV C13 in the serum (H), and amount of AST and ALT in the serum (I) of WT and *Cd11c-cre Il10*$^{fl/fl}$ mice 9 days after C13 infection and survival (%) of WT or *Cd11c-cre Il10*$^{fl/fl}$ mice after LCMV C13 infection (J). Data represent the mean ± SD of three independent experiments. *$p < 0.01$. See also Figure S7.

GAGTAACTGTGTGATTGACAAGCA-3′ (sense) and 5′-GCAGCAGTGTGT CATTCCAAGA-3′ (anti-sense); *P2y2*, 5′-CCGAGAGCTCTTTAGCCATTT-3′ (sense) and 5′-GCCATAAGCACGTAACAGACC-3′ (anti-sense); *Gapdh*, 5′-TCCACCACCCTGTTGCTGTA-3′ (sense) and 5′-ACCACAGTCCATGCCAT CAC-3′ (anti-sense); LCMV *GP*, 5′-CATTCACCTGGACTTTGTCAGACTC-3′ (sense) and 5′-GCAACTGCTGTGTTCCCGAAAC-3′ (anti-sense); LCMV *NP*, 5′-CAATGGACGCAAGCATTGAG-3′ (sense) and 5′-GTTCTTCTGCACT GAGCCTCC-3′ (anti-sense); *Mfge8*, 5′-GATCTTTCCAAC AACCT GCCT CC-3′ (sense) and 5′-ACCGCTTTCATCCTGGATGAACTC-3′ (ant-sense); *Bai1*, 5′-GCTGGCAGAAGCTGACGAT-3′ (sense) and 5′-CACGGAGATGACC TTAGAGTTG-3′ (anti-sense); *Stab2*, 5′-GCTGTCGTCCTGGTTACTG-3′ (sense) and 5′-CCAAGGCATCAATGTCATC-3′ (antisense); *Tyro3*, 5′-TGCCTG CTTCGGAACTTG-3′ (sense) and 5′-GCCTGAGTCGGTACGAATG-3′ (anti-sense); *Axl*, 5′-CCAGTCACAGGACACAGCTC-3′ (sense) and 5′-GTGACTC CCTTGGCATTG-3′ (anti-sense); *Mertk*, 5′-GGAAAGCGCAGGGACTTAC-3′ (sense) and 5′-CTGTGCAGGTGGCATTGTG-3′ (anti-sense); and *Gas6*, 5′-GGCATGTGGCAAACT ATCT-3′ (sense) and 5′-CGAGCTCACTCTCC TTGAA3′ (antisense). Primers were synthesized for *Ccr2*, *P2y2*, LCMV *GP* (Ejrnaes et al., 2006), LCMV *NP* (Djavani et al., 2001), *Mfge8*, *Bai1*, *Stab2*, *Tyro3*, *Axl*, *Mertk*, and *Gas6* by Operon Biotechnology, and for *Gapdh* by Toyobo.

Ex Vivo Hemophagocytosis Assay

TER119$^-$ Mo-DCs and TER119$^+$ erythroid cells or Gr1^{hi}Ly6c$^+$ granulocytes were separately sorted from the BM of either WT or *Mfge8*$^{-/-}$ mice at 12 hr after LCMV C13 infection. The Mo-DCs were precultured in 10% FCS-RPMI supplemented with 20 ng/ml GM-CSF, washed, then incubated with either isotype Ab cocktails (50 μg/ml of each) or blocking antibodies against Tim1, Tim4, α_v, β_3, or $\alpha_v\beta_5$ (Su et al., 2007) (50 μg/ml of each). TER119$^+$ erythroid cells were labeled with pHrodo-SE (0.5 μg/ml, Life Technologies) at room temperature for 30 min, then washed with 10% FCS PBS after stopping the reaction with 1 ml 100% FCS. To opsonize TER119$^+$ erythroid cells, the cells were incubated with goat serum at 4°C for 1 hr, washed, then incubated with anti-goat IgG antibody at 4°C for 1 hr. The Mo-DCs (4×10^4) and pHrodo-labeled erythroid cells (4×10^5), opsonized erythroid cells (4×10^5), or granulocytes (2×10^5) were cocultured in 100 μl of 10% FCS-RPMI supplemented with 20 ng/ml GM-CSF in 96 well U-bottom Ultra-Low Attached plate (Corning) at 37°C for 2 hr for Diff-Quick staining and flow cytometry or 24 hr for ELISA. To block internalization of apoptotic erythroid cells into Mo-DCs, we added control DMSO (0.01%) or cytochalasin D (5 μM) in culture for 2 hr, washed it out, then subjected 24 hr supernatants to IL-10 ELISA.

Ex Vivo Induction of PS and PS Receptors by IFN-α

Erythroid cells and granulocytes, sorted from the BM of WT mice, and T cells, B cells, NK cells, sorted from the spleen of WT mice, were stimulated ex vivo with different doses of IFN-α for 18 hr and then subjected to annexin V staining. In addition, inflammatory monocytes, sorted from the BM of WT mice, were stimulated ex vivo with IFN-α (1×10^4 U/ml) for 24 hr and then, subjected to the analysis of PS receptor expression.

Statistical Analysis

We evaluated the statistical significance of the obtained values by Student's t test. We considered a p value < 0.05 as significant.

SUPPLEMENTAL INFORMATION

Supplemental Information includes seven figures and can be found with this article online at http://dx.doi.org/10.1016/j.immuni.2013.06.019.

ACKNOWLEDGMENTS

We thank H. Kamioka for secretarial support, Shoko Kuroda for technical assistance, Nobuhiko Kamada (Keio University) for the B6.*Ccl2*$^{-/-}$ mice, Shigekazu Nagata (Kyoto University) for the B6.*Mfge8*$^{-/-}$ mice, Dean Sheppard (University of California, San Francisco) for the Ab against integrin $\alpha_v\beta_5$, Pamela S. Ohashi (Campbell Family Institute for Breast Cancer Research, Ontario Cancer Institute, University of Toronto, Toronto) for the LCMV Armstrong, and Toshitaka Akatsuka (Saitama Medical University) for the LCMV Clone 13. This work was supported by the Takeda Science Foundation (T.O.), the Joint Usage/Research Program of the Medical Research Institute, Tokyo Medical and Dental University (K.S.), a Grant-in-Aid for Scientific Research on Priority Areas from the Ministry of Education, Science, Sports and Culture of Japan (T.O.), Challenging Exploratory Research (T.O.), and Japan Science and Technology Agency, Core Research for Evolutional Science and Technology (CREST) (T.O.).

Received: September 3, 2012
Accepted: June 11, 2013
Published: September 12, 2013

REFERENCES

Akakura, S., Singh, S., Spataro, M., Akakura, R., Kim, Jong-Il., Albert, M.L., and Birge, R.B. (2003). The opsonin MFG-E8 is a ligand for the αvβ5 integrin and triggers DOCK180-dependent Rac1 activation for the phagocytosis of apoptotic cells. Exp. Cell Res. *292*, 403–416.

Atarashi, K., Tanoue, T., Shima, T., Imaoka, A., Kuwahara, T., Momose, Y., Cheng, G., Yamasaki, S., Saito, T., Ohba, Y., et al. (2011). Induction of colonic regulatory T cells by indigenous Clostridium species. Science *331*, 337–341.

Auffray, C., Sieweke, M.H., and Geissmann, F. (2009). Blood monocytes: development, heterogeneity, and relationship with dendritic cells. Annu. Rev. Immunol. *27*, 669–692.

Banchereau, J.J., Briere, F., Caux, C., Davoust, J., Lebecque, S., Liu, Y.J., Pulendran, B., and Palucka, K. (2000). Immunobiology of dendritic cells. Annu. Rev. Immunol. *18*, 767–811.

Barber, D.L., Wherry, E.J., Masopust, D., Zhu, B., Allison, J.P., Sharpe, A.H., Freeman, G.J., and Ahmed, R. (2006). Restoring function in exhausted CD8 T cells during chronic viral infection. Nature *439*, 682–687.

Behrens, E.M., Canna, S.W., Slade, K., Rao, S., Kreiger, P.A., Paessler, M., Kambayashi, T., and Koretzky, G.A. (2011). Repeated TLR9 stimulation results in macrophage activation syndrome-like disease in mice. J. Clin. Invest. *121*, 2264–2277.

Boring, L., Gosling, J., Chensue, S.W., Kunkel, S.L., Farese, R.V., Jr., Broxmeyer, H.E., and Charo, I.F. (1997). Impaired monocyte migration and reduced type 1 (Th1) cytokine responses in C-C chemokine receptor 2 knockout mice. J. Clin. Invest. *100*, 2552–2561.

Brooks, D.G., Trifilo, M.J., Edelmann, K.H., Teyton, L., McGavern, D.B., and Oldstone, M.B. (2006). Interleukin-10 determines viral clearance or persistence in vivo. Nat. Med. *12*, 1301–1309.

Budiani, D.R., Hutahaean, S., Haryana, S.M., Soesatyo, M.H., and Sosroseno, W. (2002). Interleukin-10 levels in Epstein-Barr virus-associated nasopharyngeal carcinoma. J. Microbiol. Immunol. Infect. *35*, 265–268.

Byrne, A., and Reen, D.J. (2002). Lipopolysaccharide induces rapid production of IL-10 by monocytes in the presence of apoptotic neutrophils. J. Immunol. *168*, 1968–1977.

Clark, I.A. (2007). How TNF was recognized as a key mechanism of disease. Cytokine Growth Factor Rev. *18*, 335–343.

Clerici, M., Balotta, C., Salvaggio, A., Riva, C., Trabattoni, D., Papagno, L., Berlusconi, A., Rusconi, S., Villa, M.L., Moroni, M., and Galli, M. (1996). Human immunodeficiency virus (HIV) phenotype and interleukin-2/ interleukin-10 ratio are associated markers of protection and progression in HIV infection. Blood *88*, 574–579.

Cooper, M.D., and Alder, M.N. (2006). The evolution of adaptive immune systems. Cell *124*, 815–822.

Djavani, M., Rodas, J., Lukashevich, I.S., Horejsh, D., Pandolfi, P.P., Borden, K.L., and Salvato, M.S. (2001). Role of the promyelocytic leukemia protein PML in the interferon sensitivity of lymphocytic choriomeningitis virus. J. Virol. *75*, 6204–6208.

Domínguez, P.M., and Ardavín, C. (2010). Differentiation and function of mouse monocyte-derived dendritic cells in steady state and inflammation. Immunol. Rev. *234*, 90–104.

Ejrnaes, M., Filippi, C.M., Martinic, M.M., Ling, E.M., Togher, L.M., Crotty, S., and von Herrath, M.G. (2006). Resolution of a chronic viral infection after interleukin-10 receptor blockade. J. Exp. Med. *203*, 2461–2472.

Elliott, M.R., Chekeni, F.B., Trampont, P.C., Lazarowski, E.R., Kadl, A., Walk, S.F., Park, D., Woodson, R.I., Ostankovich, M., Sharma, P., et al. (2009). Nucleotides released by apoptotic cells act as a find-me signal to promote phagocytic clearance. Nature *461*, 282–286.

Geissmann, F., Manz, M.G., Jung, S., Sieweke, M.H., Merad, M., and Ley, K. (2010). Development of monocytes, macrophages, and dendritic cells. Science *327*, 656–661.

Hanayama, R., Tanaka, M., Miwa, K., Shinohara, A., Iwamatsu, A., and Nagata, S. (2002). Identification of a factor that links apoptotic cells to phagocytes. Nature *417*, 182–187.

Hanayama, R., Tanaka, M., Miyasaka, K., Aozasa, K., Koike, M., Uchiyama, Y., and Nagata, S. (2004). Autoimmune disease and impaired uptake of apoptotic cells in MFG-E8-deficient mice. Science *304*, 1147–1150.

Janka, G.E. (2007). Hemophagocytic syndromes. Blood Rev. *21*, 245–253.

Jung, S., Aliberti, J., Graemmel, P., Sunshine, M.J., Kreutzberg, G.W., Sher, A., and Littman, D.R. (2000). Analysis of fractalkine receptor $CX_{(3)}CR1$ function by targeted deletion and green fluorescent protein reporter gene insertion. Mol. Cell. Biol. *20*, 4106–4114.

Kawai, T., and Akira, S. (2010). The role of pattern-recognition receptors in innate immunity: update on Toll-like receptors. Nat. Immunol. *11*, 373–384.

Kawane, K., Fukuyama, H., Kondoh, G., Takeda, J., Ohsawa, Y., Uchiyama, Y., and Nagata, S. (2001). Requirement of DNase II for definitive erythropoiesis in the mouse fetal liver. Science *292*, 1546–1549.

Kim, S., Elkon, K.B., and Ma, X. (2004). Transcriptional suppression of interleukin-12 gene expression following phagocytosis of apoptotic cells. Immunity *21*, 643–653.

Kobasa, D., Jones, S.M., Shinya, K., Kash, J.C., Copps, J., Ebihara, H., Hatta, Y., Kim, J.H., Halfmann, P., Hatta, M., et al. (2007). Aberrant innate immune response in lethal infection of macaques with the 1918 influenza virus. Nature *445*, 319–323.

Kobayashi, N., Karisola, P., Peña-Cruz, V., Dorfman, D.M., Jinushi, M., Umetsu, S.E., Butte, M.J., Nagumo, H., Chernova, I., Zhu, B., et al. (2007). TIM-1 and TIM-4 glycoproteins bind phosphatidylserine and mediate uptake of apoptotic cells. Immunity *27*, 927–940.

Lambeth, J.D. (2007). Nox enzymes, ROS, and chronic disease: an example of antagonistic pleiotropy. Free Radic. Biol. Med. *43*, 332–347.

Larroche, C., and Mouthon, L. (2004). Pathogenesis of hemophagocytic syndrome (HPS). Autoimmun. Rev. *3*, 69–75.

León, B., López-Bravo, M., and Ardavín, C. (2007). Monocyte-derived dendritic cells formed at the infection site control the induction of protective T helper 1 responses against Leishmania. Immunity *26*, 519–531.

Lu, B., Rutledge, B.J., Gu, L., Fiorillo, J., Lukacs, N.W., Kunkel, S.L., North, R., Gerard, C., and Rollins, B.J. (1998). Abnormalities in monocyte recruitment and cytokine expression in monocyte chemoattractant protein 1-deficient mice. J. Exp. Med. *187*, 601–608.

Maakaroun, N.R., Moanna, A., Jacob, J.T., and Albrecht, H. (2010). Viral infections associated with haemophagocytic syndrome. Rev. Med. Virol. *20*, 93–105.

Martin, S.J., Finucane, D.M., Amarante-Mendes, G.P., O'Brien, G.A., and Green, D.R. (1996). Phosphatidylserine externalization during CD95-induced apoptosis of cells and cytoplasts requires ICE/CED-3 protease activity. J. Biol. Chem. *271*, 28753–28756.

Matloubian, M., Somasundaram, T., Kolhekar, S.R., Selvakumar, R., and Ahmed, R. (1990). Genetic basis of viral persistence: single amino acid change in the viral glycoprotein affects ability of lymphocytic choriomeningitis virus to persist in adult mice. J. Exp. Med. *172*, 1043–1048.

Medzhitov, R., and Janeway, C.A., Jr. (1997). Innate immunity: the virtues of a nonclonal system of recognition. Cell *91*, 295–298.

Miyanishi, M., Tada, K., Koike, M., Uchiyama, Y., Kitamura, T., and Nagata, S. (2007). Identification of Tim4 as a phosphatidylserine receptor. Nature *450*, 435–439.

Nagata, S., Hanayama, R., and Kawane, K. (2010). Autoimmunity and the clearance of dead cells. Cell *140*, 619–630.

Nakayama, M., Akiba, H., Takeda, K., Kojima, Y., Hashiguchi, M., Azuma, M., Yagita, H., and Okumura, K. (2009). Tim-3 mediates phagocytosis of apoptotic cells and cross-presentation. Blood *113*, 3821–3830.

Nordøy, I., Müller, F., Nordal, K.P., Rollag, H., Lien, E., Aukrust, P., and Froland, S.S. (2000). The role of the tumor necrosis factor system and interleukin-10 during cytomegalovirus infection in renal transplant recipients. J. Infect. Dis. *181*, 51–57.

Randolph, G.J., Inaba, K., Robbiani, D.F., Steinman, R.M., and Muller, W.A. (1999). Differentiation of phagocytic monocytes into lymph node dendritic cells in vivo. Immunity *11*, 753–761.

Rodriguez-Manzanet, R., Meyers, J.H., Balasubramanian, S., Slavik, J., Kassam, N., Dardalhon, V., Greenfield, E.A., Anderson, A.C., Sobel, R.A., Hafler, D.A., et al. (2008). TIM-4 expressed on APCs induces T cell expansion and survival. J. Immunol. *180*, 4706–4713.

Roers, A., Siewe, L., Strittmatter, E., Deckert, M., Schlüter, D., Stenzel, W., Gruber, A.D., Krieg, T., Rajewsky, K., and Müller, W. (2004). T cell-specific inactivation of the interleukin 10 gene in mice results in enhanced T cell responses but normal innate responses to lipopolysaccharide or skin irritation. J. Exp. Med. *200*, 1289–1297.

Rouse, B.T., and Sehrawat, S. (2010). Immunity and immunopathology to viruses: what decides the outcome? Nat. Rev. Immunol. *10*, 514–526.

Schaer, C.A., Schoedon, G., Imhof, A., Kurrer, M.O., and Schaer, D.J. (2006a). Constitutive endocytosis of CD163 mediates hemoglobin-heme uptake and determines the noninflammatory and protective transcriptional response of macrophages to hemoglobin. Circ. Res. *99*, 943–950.

Schaer, D.J., Schaer, C.A., Schoedon, G., Imhof, A., and Kurrer, M.O. (2006b). Hemophagocytic macrophages constitute a major compartment of heme oxygenase expression in sepsis. Eur. J. Haematol. *77*, 432–436.

Schneider, D.S., and Ayres, J.S. (2008). Two ways to survive infection: what resistance and tolerance can teach us about treating infectious diseases. Nat. Rev. Immunol. *8*, 889–895.

Serbina, N.V., and Pamer, E.G. (2006). Monocyte emigration from bone marrow during bacterial infection requires signals mediated by chemokine receptor CCR2. Nat. Immunol. *7*, 311–317.

Serbina, N.V., Jia, T., Hohl, T.M., and Pamer, E.G. (2008). Monocyte-mediated defense against microbial pathogens. Annu. Rev. Immunol. *26*, 421–452.

Sevilla, N., Kunz, S., Holz, A., Lewicki, H., Homann, D., Yamada, H., Campbell, K.P., de La Torre, J.C., and Oldstone, M.B. (2000). Immunosuppression and resultant viral persistence by specific viral targeting of dendritic cells. J. Exp. Med. *192*, 1249–1260.

Stranges, P.B., Watson, J., Cooper, C.J., Choisy-Rossi, C.M., Stonebraker, A.C., Beighton, R.A., Hartig, H., Sundberg, J.P., Servick, S., Kaufmann, G., et al. (2007). Elimination of antigen-presenting cells and autoreactive T cells by Fas contributes to prevention of autoimmunity. Immunity *26*, 629–641.

Su, G., Hodnett, M., Wu, N., Atakilit, A., Kosinski, C., Godzich, M., Huang, X.Z., Kim, J.K., Frank, J.A., Matthay, M.A., et al. (2007). Integrin alphavbeta5 regulates lung vascular permeability and pulmonary endothelial barrier function. Am. J. Respir. Cell Mol. Biol. *36*, 377–386.

Takahashi, K., Nakamura, T., Koyanagi, M., Kato, K., Hashimoto, Y., Yagita, H., and Okumura, K. (1990). A murine very late activation antigen-like extracellular matrix receptor involved in CD2- and lymphocyte function-associated antigen-1-independent killer-target cell interaction. J. Immunol. *145*, 4371–4379.

Tarumi, T., Sawada, K., Sato, N., Kobayashi, S., Takano, H., Yasukouchi, T., Takashashi, T., Sekiguchi, S., and Koike, T. (1995). Interferon-α-induced apoptosis in human erythroid progenitors. Exp. Hematol. *23*, 1310–1318.

Voll, R.E., Herrmann, M., Roth, E.A., Stach, C., Kalden, J.R., and Girkontaite, I. (1997). Immunosuppressive effects of apoptotic cells. Nature *390*, 350–351.

Waibler, Z., Anzaghe, M., Konur, A., Akira, S., Müller, W., and Kalinke, U. (2008). Excessive CpG 1668 stimulation triggers IL-10 production by cDC that inhibits IFN-α responses by pDC. Eur. J. Immunol. *38*, 3127–3137.

Xiao, S., Najafian, N., Reddy, J., Albin, M., Zhu, C., Jensen, E., Imitola, J., Korn, T., Anderson, A.C., Zhang, Z., et al. (2007). Differential engagement of Tim-1 during activation can positively or negatively costimulate T cell expansion and effector function. J. Exp. Med. *204*, 1691–1702.

Xiao, S., Zhu, B., Jin, H., Zhu, C., Umetsu, D.T., DeKruyff, R.H., and Kuchroo, V.K. (2011). Tim-1 stimulation of dendritic cells regulates the balance between effector and regulatory T cells. Eur. J. Immunol. *41*, 1539–1549.

Yasuda, M., Hasunuma, Y., Adachi, H., Sekine, C., Sakanishi, T., Hashimoto, H., Ra, C., Yagita, H., and Okumura, K. (1995). Expression and function of fibronectin binding integrins on rat mast cells. Int. Immunol. *7*, 251–258.

Yoshida, H., Okabe, Y., Kawane, K., Fukuyama, H., and Nagata, S. (2005). Lethal anemia caused by interferon-β produced in mouse embryos carrying undigested DNA. Nat. Immunol. *6*, 49–56.

Zinkernagel, R.M., Haenseler, E., Leist, T., Cerny, A., Hengartner, H., and Althage, A. (1986). T cell-mediated hepatitis in mice infected with lymphocytic choriomeningitis virus. Liver cell destruction by H-2 class I-restricted virus-specific cytotoxic T cells as a physiological correlate of the ^{51}Cr-release assay? J. Exp. Med. *164*, 1075–1092.

Zoller, E.E., Lykens, J.E., Terrell, C.E., Aliberti, J., Filipovich, A.H., Henson, P.M., and Jordan, M.B. (2011). Hemophagocytosis causes a consumptive anemia of inflammation. J. Exp. Med. *208*, 1203–1214.

CME/SAM

Correlation Between Dysplastic Lineage and Type of Cytopenia in Myelodysplastic Syndromes Patients With Refractory Anemia According to the FAB Classification

Akira Matsuda, MD,[1] Itsuro Jinnai, MD,[1] Masako Iwanaga, MD, PhD,[2] Daisuke Okamura, MD,[1] Maho Ishikawa, MD,[1] Tomoya Maeda, MD,[1] Tomoko Hata, MD,[2] Nobutaka Kawai, MD,[1] Yasushi Miyazaki, MD,[2] Masami Bessho, MD,[1] and Masao Tomonaga, MD[3]

From the [1]Department of Hemato-Oncology, Saitama International Medical Center, Saitama Medical University, Saitama, Japan; [2]Department of Hematology, Molecular Medicine Unit, Atomic Bomb Disease Institute, Nagasaki University Graduate School of Biomedical Sciences, Nagasaki, Japan; and [3]Department of Hematology, Japanese Red Cross Nagasaki Atomic Bomb Hospital, Nagasaki, Japan.

Key Words: Myelodysplastic syndromes; Cytopenia; Dysplastic features; WHO classification

DOI: 10.1309/AJCPJEFPNTMM3KSH

ABSTRACT

Objectives: *To analyze the correlation between dysplastic lineage and type of cytopenia in myelodysplastic syndromes.*

Methods: *We analyzed the correlation between dysplasia and cell count using the data set of our previous morphologic study.*

Results: *There were no correlations between dysgranulopoiesis of 10% or more and absolute neutrophil count (ANC). Similarly, hyposegmented mature neutrophils (Pelger) of 10% or more were not related to ANC. Interestingly, the platelet count of patients with dysmegakaryopoiesis (dys Mgk) was higher than that of patients without dys Mgk (dys Mgk ≥10% vs <10%,* P = *.08; dys Mgk ≥40% vs <40%,* P = *.02; micromegakaryocytes ≥10% vs <10%,* P = *.004).*

Conclusions: *Since low cell counts did not correlate with the presence of dysplastic features, we suggest that dysplastic features do not directly relate to apoptosis.*

Upon completion of this activity you will be able to:
- list the dysplasia(s) in bone marrow for diagnosis of myelodysplastic syndromes (MDS).
- describe the mechanism of cytopenia(s) in MDS patients.
- define MDS subtypes according to 2008 World Health Organization criteria.

The ASCP is accredited by the Accreditation Council for Continuing Medical Education to provide continuing medical education for physicians. The ASCP designates this journal-based CME activity for a maximum of 1 *AMA PRA Category 1 Credit*™ per article. Physicians should claim only the credit commensurate with the extent of their participation in the activity. This activity qualifies as an American Board of Pathology Maintenance of Certification Part II Self-Assessment Module.

The authors of this article and the planning committee members and staff have no relevant financial relationships with commercial interests to disclose.

Questions appear on p 277. Exam is located at www.ascp.org/ajcpcme.

Myelodysplastic syndromes (MDS) are very heterogeneous in terms of their cytomorphology, clinical features, and survival.[1] In 1982, the French-American-British (FAB) classification for the diagnosis of MDS was proposed,[2] and the current World Health Organization (WHO) classification[3] was proposed in 2008. The chapter on refractory cytopenia with unilineage dysplasia of the WHO classification described that "the type of cytopenia in the majority of cases will correspond to the type of dysplasia, e.g. anemia and erythroid dysplasia."[4] Although many groups have reported the cytomorphologic findings of MDS, to our knowledge a detailed analysis of the relationship between dysplastic lineage and the type of cytopenia has not been completely studied. Therefore, the correlation between dysplastic lineage and the type of cytopenia is unclear. Patients with MDS who do not exhibit a correlation between dysplastic lineage and the type of

cytopenia certainly exist. For example, MDS associated with isolated del(5q) (5q– syndrome) shows remarkable dysplastic features of megakaryocytic lineage in bone marrow (BM). However, the platelet counts of patients with 5q– syndrome do not usually decrease.[3] Previously, we reported a detailed cytomorphologic analysis of refractory anemia according to the FAB classification (FAB-RA).[5] Using this data set, we analyzed the relationship between dysplastic lineage and cell count in the present study.

Table 1
Patient Characteristics

Characteristic	Value
Age, median (range), y	57 (15-88)
Male sex, No. (%)	53 (53)
Hb, median (range), g/dL	8.3 (2.9-14.3)
ANC, median (range), $\times 10^9$/L	1.397 (0.260-6.201)
PLT, median (range), $\times 10^9$/L	35 (4-760)
Chromosome (IPSS), No. (%)	
Good	76 (76)
Intermediate	15 (15)
Poor	9 (9)

ANC, absolute neutrophil count; Hb, hemoglobin; IPSS, International Prognostic Scoring System; PLT, platelet count.

Materials and Methods

Patients

The data set of Japanese patients from our previous study[5] was used for this study. Patients included those with primary MDS excluding refractory anemia with ringed sideroblasts, refractory cytopenia with multilineage dysplasia and ringed sideroblasts, refractory anemia with excess of blasts (RAEB), or 5q– syndrome according to WHO classification (version 3).[6] Therefore, all patients in this study had FAB-RA except those with 5q– syndrome. Patients were diagnosed at the Saitama Medical University Hospital, Nagasaki University Hospital, or affiliated hospitals between April 1976 and January 2002. BM cellularity and fibrosis were evaluated by BM trephine biopsy and/or clot section. Patients with BM fibrosis were excluded, because the accuracy of morphologic evaluations might be not reliable owing to the few BM cells of the films. Disorders other than MDS (eg, aplastic anemia, paroxysmal nocturnal hemoglobinuria, megaloblastic anemia, autoimmune hemolytic anemia, anemia of chronic disorders, large granular lymphocytic leukemia, hairy cell leukemia, chronic liver disorders, and hypersplenism) were excluded. Patients who had previous therapy (antineoplastic drugs and/or ionizing radiation) or other prior hematologic disease also were excluded from the study. This study was approved by the Institutional Review Board of Saitama International Medical Center, Saitama Medical University. Retrospective analysis was performed in 100 Japanese patients. Age, sex, and cytogenetic findings of patients at diagnosis are summarized in **Table 1**.

Cytomorphologic Study

Microscopic examinations were performed using standard methods (BM Wright-Giemsa [WG] or May-Giemsa [MG], Prussian blue and periodic acid–Schiff [PAS] stained films, and peripheral blood [PB] WG- or MG-stained films).

In the present study, we analyzed the correlation between dysplasia and cell count using the data set of our previous morphologic study, in which we performed a detailed cytomorphologic analysis. We limited dysplasias to only dysplasias described in the WHO classification (version 3)[6] as follows. Dysplasias of the nucleus in erythroid lineage cells were defined as having budding, bridging, internuclear, karyorrhexis, multinuclearity, or megaloblastoid changes. Dysplasias of the cytoplasm in erythroid lineage cells were defined as having ring sideroblasts, vacuolization, or PAS positivity (diffuse or granular). With regard to granulocytes, dysplasias were defined as having the following characteristics: small size, nuclear hyposegmented mature neutrophils (Pelger), hypersegmentation, hypogranularity, or pseudo–Chédiak-Higashi granules. Dysplasias of megakaryocytes were defined as having micromegakaryocytes (mMgk), nonlobulated nuclei, or multiple widely separated nuclei. A minimum of 25 megakaryocytes, 200 erythroblasts, and 200 neutrophils in BM were examined in each patient. The cutoff levels for dyserythropoiesis (dys E) and dysgranulopoiesis (dys G) were defined as 10% according to the WHO classification.[6] Dysmegakaryopoiesis (dys Mgk) was evaluated with 2 cutoff levels: 10% according to the WHO classification or 40% according to data previously reported from the German group.[7,8] Since the accuracy of the quantitative evaluation of dysmegakaryopoiesis might be not reliable when there are few megakaryocytes to examine, we excluded patients who did not have at least 25 examined megakaryocytes from the morphologic evaluation of the megakaryocytic lineage. In our previous study, we reported that 2 distinct dysplastic changes, Pelger and mMgk **Image 1**, had negative prognostic impacts. Therefore, Pelger and mMgk were also evaluated. We defined hyposegmented mature neutrophils with strikingly clumpy chromatin as "Pelger" and mononucleated or binucleated megakaryocytes with a size equal to or smaller than promyelocytes as "mMgk." Positivity for Pelger (Pelger+) was defined as the presence of 10% or more Pelger among 200 mature neutrophils. Positivity for mMgk (mMgk+) was defined as the presence of 10% or more mMgk among 25 or more megakaryocytes. Patients with decreased megakaryocytes were assessed as being negative for mMgk (mMgk–).

DOI: 10.1309/AJCPJEFPNTMM3KSH

Definition of Cytopenias

To analyze the relationship between dysplasia and cytopenia, we compared hemoglobin (Hb) concentrations, absolute neutrophil counts (ANCs), platelet counts, and types of cytopenia. The definitions of cytopenias were as follows: Hb concentration less than 10 g/dL, ANC less than 1.8×10^9/L, and platelet count less than 100×10^9/L.[3]

Statistical Analysis

Continuous data were compared using the nonparametric Mann-Whitney test, and proportions were compared using the χ^2 test. A 2-sided *P* value of less than .05 was considered statistically significant.

Results

Cytomorphologic Study

In our previous data set, we evaluated suitable BM preparations for the detailed assessments of myelodysplasia.[5] Results of morphologic analysis are shown in **Table 2** and **Table 3**. Some BM preparations could not be examined in detail. In particular, observing the granules of neutrophils was difficult due to the poor staining condition of the films. Four cases could not be evaluated for the frequency of dys G, and 1 case could not be evaluated for the frequency of Pelger. Nineteen patients showed decreased megakaryocytes. Therefore,

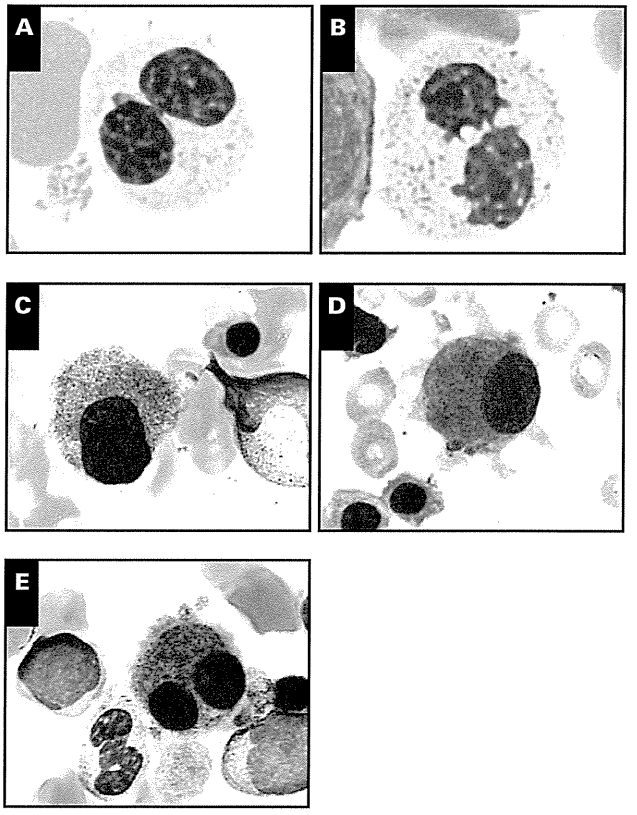

Image 1 **A** and **B**, Nuclear hyposegmented mature neutrophils (Pelger) (May-Giemsa). **C-E**, Micromegakaryocytes (May-Giemsa).

Table 2
Relationship Between Dysgranulopoiesis and Absolute Neutrophil Count

Characteristic	No. of Patients	ANC, Median (Range), $\times 10^9$/L	*P* Value	No. (%) of Patients With Neutropenia[a]	*P* Value
dys G ≥10%	17	1.394 (0.492-6.201)	.83	13 (76.5)	.22
dys G <10%	79	1.397 (0.260-4.708)		48 (60.8)	
Pelger ≥10%	12	1.364 (0.492-6.201)	.86	9 (75.0)	.42
Pelger <10%	87	1.394 (0.260-4.708)		55 (63.2)	

ANC, absolute neutrophil count; dys G, dysgranulopoiesis; Pelger, nuclear hyposegmented mature neutrophils.
[a] Definition of neutropenia is ANC $<1.8 \times 10^9$/L.

Table 3
Relationship Between Dysmegakaryopoiesis and Platelet Count

Characteristic	No. of Patients	Platelets, Median (Range), $\times 10^9$/L	*P* Value	No. (%) of Patients With Thrombocytopenia[a]	*P* Value
dys Mgk ≥10%	69	48 (8-760)	.08	51 (73.9)	.18
dys Mgk <10%	12	26 (5-313)		11 (91.7)	
dys Mgk ≥40%	38	70 (15-760)	.02	26 (68.4)	.10
dys Mgk <40%	43	36 (5-343)		36 (83.7)	
mMgk ≥10%	12	99 (29-760)	.004	7 (58.3)	.03
mMgk <10%	88	33 (4-390)		7 (84.1)	

dys Mgk, dysmegakaryopoiesis; mMgk, micromegakaryocytes.
[a] Definition of thrombocytopenia is platelet count $<100 \times 10^9$/L.

DOI: 10.1309/AJCPJEFPNTMM3KSH

these cases could not be evaluated for the frequency of dys Mgk. All patients showed dys E of 10% or more. No patients with unilineage dysplasia had dys G or dys Mgk of 10% or more. Patients with unilineage dysplasia had an erythroid lineage. Seventeen (18%) and 12 (12%) patients had dys G of 10% or more and were Pelger+, respectively. Sixty-nine (85%) and 38 (47%) patients had dys Mgk of 10% or more and 40% or more, respectively. Twelve (12%) patients were mMgk+. All patients with mMgk+ showed dys Mgk of 40% or more.

Table 4
Dysplastic Lineage(s) in Patients With Unilineage Cytopenia[a]

Case No.	dys E ≥10%	dys G ≥10%	dys Mgk ≥10%
Patients with only anemia			
103	+	−	+
131	+	+	−
136	+	−	+
257	+	−	+
Patients with only neutropenia			
135	+	+	+
230	+	+	+
245	+	−	+
286	+	−	+
Patients with only thrombocytopenia			
129	+	−	−
154	+	−	+
233	+	−	+
248	+	−	Unknown[b]
252	+	−	−
269	+	−	+
270	+	+	+
271	+	−	+
273	+	−	+
278	+	−	+
290	+	−	+

dys E, dyserythropoiesis; dys G, dysgranulopoiesis; dys Mgk, dysmegakaryopoiesis.
[a] Definitions of cytopenias are hemoglobin concentration <10 g/dL, absolute neutrophil count <1.8 × 10^9/L, and platelet count <100 × 10^9/L.
[b] Could not be evaluated for the frequency of dys Mgk due to decreases in megakaryocytes.

Table 5
Relationship Between Dysplastic Lineage and the Type of Cytopenia in Patients With Unilineage Dysplasia[a]

Case No.	Dysplastic Lineage	Anemia	Neutropenia	Thrombocytopenia
109	Erythroid	+	+	+
120	Erythroid	−	+	+
125	Erythroid	+	+	+
127	Erythroid	−	+	+
129	Erythroid	−	−	+
134	Erythroid	+	−	+
140	Erythroid	+	−	+
202	Erythroid	+	+	+
204	Erythroid	+	+	+
236	Erythroid	+	+	+
252	Erythroid	−	−	+

[a] Definitions of cytopenias are hemoglobin concentration <10g/dL, absolute neutrophil count <1.8 × 10^9/L, and platelet count <100 × 10^9/L.

Relationship Between Dysplasia and Cell Count

Results of the relationship between dysplasia and cell count are shown in Tables 2 and 3. There was no relationship between the presence of dys G of 10% or more and ANC. Similarly, Pelger+ was not related to ANC. Interestingly, platelet counts of patients with dys Mgk of 10% or more tended to be higher than those of patients without dys Mgk of 10% or more ($P = .08$). Moreover, in patients with dys Mgk of 40% or more, this difference in platelet counts was significant (dys Mgk ≥40% vs <40%, $P = .02$). In particular, in patients with mMgk+, the sign became even clearer ($P = .004$). In patients with dys Mgk of 40% or more, the platelet count of those with mMgk+ was not different from those without mMgk+ ($P = .47$). Of the 19 patients who showed unilineage cytopenia, only 2 had unilineage dysplasia. However, dysplastic lineages were different from the lineages of cytopenia **Table 4**. Of the 11 patients who showed unilineage dysplasia, only 2 had unilineage cytopenia. However, lineages of cytopenia were different from dysplastic lineages **Table 5**.

Discussion

Generally, it seems that cytopenias correspond to dysplastic lineage, but this has not been studied completely. Increases in blasts in BM may reduce blood cell counts due to hematopoietic injury. Patients with 5q– syndrome show anemia due to erythroid hypoplasia.[9,10] Increases in blasts or the existence of del(5q) may influence the decrease in cell count. To examine the correct relationship between dysplastic lineage and cell count, we excluded patients with RAEB or 5q– syndrome. Our previous data set used for the present study also does not include these cases. Therefore, it seems that this data set is suitable for the purpose of the present study.

Recently, it was reported that there was no clear correlation between the presence of any distinct dysplastic sign and cell counts in patients with MDS.[11] In the present study, we could not find any correlation between the presence of dys G of 10% or more and ANC. Low ANC cannot be directly explained by the presence of dys G. This result suggests that dysplastic features in granulocytic lineage may be unrelated to ineffective hematopoiesis explained by apoptosis. Interestingly, the platelet count of patients with dys Mgk was higher than that of patients without dys Mgk (dys Mgk ≥10% vs <10%, $P = .08$; dys Mgk ≥40% vs <40%, $P = .02$; mMgk+ vs mMgk–, $P = .004$). Although patients with 5q– syndrome show remarkable dysplastic features of megakaryocytic lineage in BM, their platelet counts are usually normal or increased. Thrombocytopenia is uncommon.[3,9,10] In the present study, a correlation between dys Mgk and platelet counts was similar to the characteristics of 5q– syndrome. These findings suggest that dys Mgk is not related to a direct sign of apoptosis, at least in the megakaryocytic lineage. In addition, we analyzed

DOI: 10.1309/AJCPJEFPNTMM3KSH

the correlation between the frequency of dys Mgk and the number of megakaryocytes. Evaluation of the megakaryocyte count was performed using specimens of the BM trephine biopsy and/or clot section. Of the 38 patients with dys Mgk of 40% or more, 21 (55%), 10 (26%), and 7 (17%) had increased, normal, and decreased megakaryocyte counts, respectively. In patients with dys Mgk of 40% or more, megakaryocyte counts tended to increase. In contrast, of the 43 patients without dys Mgk of 40% or more, 5 (12%), 17 (40%), and 21 (48%) had increased, normal, and decreased megakaryocyte counts, respectively. In patients without dys Mgk of 40% or more, megakaryocyte counts did not tend to increase. This finding was similar to a correlation between megakaryocyte count and mMgk. In 12 patients with mMgk+, 9 (75%), 3 (25%), and 0 had increased, normal, and decreased megakaryocyte counts, respectively. In patients with mMgk+, megakaryocyte counts tended to increase. In contrast, of the 88 patients without dys mMgk+, 17 (19%), 24 (27%), and 47 (53%) had increased, normal, and decreased megakaryocyte counts, respectively. In patients without mMgk+, megakaryocyte counts did not tend to increase. Increases in megakaryocyte counts may be a reason for the increase in platelet counts in patients with dys Mgk of 40% or more or mMgk+.

Only 6 patients had hypoplastic BM. There was no significant difference in Hb concentrations between hypoplastic BM and nonhypoplastic BM patients ($P = .51$). Similarly, there was no significant difference in ANC between the 2 groups ($P = .44$). Nineteen patients had decreased megakaryocytes. Interestingly, the platelet count of patients with decreased megakaryocytes (median, 18×10^9/L) was significantly lower than that of patients without decreased megakaryocytes (median, 48×10^9/L) ($P < .001$). This finding is similar to the mechanism of thrombocytopenia in patients with aplastic anemia. It seems that the presence of decreased megakaryocytes may be associated with the presence of thrombocytopenia even in patients with MDS.

We could not find a correlation between dysplastic lineage and low cell counts. Low ANC cannot be explained by the presence of dys G. The platelet count of patients with dys Mgk was higher than that of patients without dys Mgk. Therefore, we suggest that dysplastic features do not directly relate to apoptosis in MDS patients with FAB-RA except 5q– syndrome. To clarify the conclusion of our study, quantitative analysis of apoptosis by immunohistochemistry should be performed in the future studies.

Address reprint requests to Dr Matsuda: Dept of Hematology, Saitama International Medical Center, Saitama Medical University, 1397-1 Yamane, Hidaka, Saitama, 350-1298, Japan; e-mail: amatsu@saitama-med.ac.jp.

References

1. Malcovati L, Porta MG, Pascutto C, et al. Prognostic factors and life expectancy in myelodysplastic syndromes classified according to WHO criteria: a basis for clinical decision-making. *J Clin Oncol*. 2005;23:7594-7603.
2. Bennett JM, Catovsky D, Daniel MT, et al. Proposals for the classification of the myelodysplastic syndromes. *Br J Haematol*. 1982;51:189-199.
3. Brunning RD, Orazi A, Germing U, et al. Myelodysplastic syndromes/neoplasms, overview. In: Swerdlow SH, Campo E, Harris NL, et al, eds. *WHO Classification of Tumours of Haematopoietic and Lymphoid Tissues*. Lyon, France: IARC Press; 2008:88-93.
4. Brunning RD, Hasserjian RP, Porwit A, et al. Refractory cytopenia with unilineage dysplasia. In: Swerdlow SH, Campo E, Harris NL, et al, eds. *WHO Classification of Tumours of Haematopoietic and Lymphoid Tissues*. Lyon, France: IARC Press; 2008:94-95.
5. Matsuda A, Germing U, Jinnai I, et al. Improvement of criteria for refractory cytopenia with multilineage dysplasia according to the WHO classification based on prognostic significance of morphological features in patients with refractory anemia according to the FAB classification. *Leukemia*. 2007;21:678-686.
6. Brunning RD, Bennet JM, Flandrin G, et al. WHO histological classification of myelodysplastic syndromes. In: Jaffe ES, Harris NL, Stein H, et al, eds. *World Health Organization Classification of Tumours: Pathology and Genetics of Tumour of Haematopoietic and Lymphoid Tissues*. Lyon, France: IARC Press; 2001:62-73.
7. Germing U, Gattermann N, Strupp C, et al. Validation of the WHO proposals for a new classification of primary myelodysplastic syndromes: a retrospective analysis of 1600 patients. *Leuk Res*. 2000;24:983-992.
8. Germing U, Gattermann N, Aivado M, et al. Two types of acquired idiopathic sideroblastic anaemia (AISA): a time-tested distinction. *Br J Haematol*. 2000;108:724-728.
9. Cazzola M. Myelodysplastic syndrome with isolated 5q deletion (5q- syndrome): a clonal stem cell disorder characterized by defective ribosome biogenesis. *Haematologica*. 2008;93:967-972.
10. Boultwood J, Lewis S, Wainscoat JS. The 5q-syndrome. *Blood*. 1994;84:3253-3260.
11. Germing U, Strupp C, Giagounidis A, et al. Evaluation of dysplasia through detailed cytomorphology in 3156 patients from the Düsseldorf Registry on myelodysplastic syndromes. *Leuk Res*. 2012;36:727-734.

DOI: 10.1309/AJCPJEFPNTMM3KSH

TLL performed the plasma cytokine profiling. CAH provided hematopathology review. All authors approved the final version of the paper for submission.

A Pardanani[1], C Finke[1], RA Abdelrahman[1], TL Lasho[1], CA Hanson[2] and A Tefferi[1]
[1]*Division of Hematology, Department of Medicine, Mayo Clinic, Rochester, MN, USA and*
[2]*Division of Hematopathology, Department of Laboratory Medicine and Pathology, Mayo Clinic, Rochester, MN, USA*
E-mail: Pardanani.animesh@mayo.edu

REFERENCES

1 Horny HP, Metcalfe DD, Bennett JM, Bain BJ, Akin C, Escribano L *et al.* Mastocytosis. In: Swerdlow SH, Campo E, Harris NL, Jaffe ES, Pileri SA, Stein H *et al.* (eds) *WHO Classification of Tumors of Hematopoietic and Lymphoid Tissues*. 4th edn. (International Agency for Research and Cancer (IARC): Lyon, 2008, pp 54–63.
2 Lim KH, Tefferi A, Lasho TL, Finke C, Patnaik M, Butterfield JH *et al.* Systemic mastocytosis in 342 consecutive adults: survival studies and prognostic factors. *Blood* 2009; **113**: 5727–5736.
3 Escribano L, Alvarez-Twose I, Sanchez-Munoz L, Garcia-Montero A, Nunez R, Almeida J *et al.* Prognosis in adult indolent systemic mastocytosis: a long-term study of the Spanish Network on Mastocytosis in a series of 145 patients. *J Allergy Clin Immunol* 2009; **124**: 514–521.
4 Pardanani A, Lim KH, Lasho TL, Finke CM, McClure RF, Li CY *et al.* WHO subvariants of indolent mastocytosis: clinical details and prognostic evaluation in 159 consecutive adults. *Blood* 2010; **115**: 150–151.
5 Tefferi A, Vaidya R, Caramazza D, Finke C, Lasho T, Pardanani A. Circulating interleukin (IL)-8, IL-2R, IL-12, and IL-15 levels are independently prognostic in primary myelofibrosis: a comprehensive cytokine profiling study. *J Clin Oncol* 2011; **29**: 1356–1363.
6 Pardanani A, Finke C, Lasho TL, Al-Kali A, Begna KH, Hanson CA *et al.* IPSS-independent prognostic value of plasma CXCL10, IL-7 and IL-6 levels in myelodysplastic syndromes. *Leukemia* 2012; **26**: 693–699.
7 Ansell SM, Maurer MJ, Ziesmer SC, Slager SL, Habermann TM, Link BK *et al.* Elevated pretreatment serum levels of interferon-inducible protein-10 (CXCL10) predict disease relapse and prognosis in diffuse large B-cell lymphoma patients. *Am J Hematol* 2012; **87**: 865–869.
8 Vardiman JW, Thiele J, Arber DA, Brunning RD, Borowitz MJ, Porwit A *et al.* The 2008 revision of the World Health Organization (WHO) classification of myeloid neoplasms and acute leukemia: rationale and important changes. *Blood* 2009; **114**: 937–951.
9 Akin C, Schwartz LB, Kitoh T, Obayashi H, Worobec AS, Scott LM *et al.* Soluble stem cell factor receptor (CD117) and IL-2 receptor alpha chain (CD25) levels in the plasma of patients with mastocytosis: relationships to disease severity and bone marrow pathology. *Blood* 2000; **96**: 1267–1273.
10 Morgado JM, Sanchez-Munoz L, Teodosio CG, Jara-Acevedo M, Alvarez-Twose I, Matito A *et al.* Immunophenotyping in systemic mastocytosis diagnosis: 'CD25 positive' alone is more informative than the 'CD25 and/or CD2' WHO criterion. *Mod Pathol* 2012; **25**: 516–521.
11 Olejniczak K, Kasprzak A. Biological properties of interleukin 2 and its role in pathogenesis of selected diseases--a review. *Med Sci Monit* 2008; **14**: RA179–RA189.
12 Horny HP, Sotlar K, Sperr WR, Valent P. Systemic mastocytosis with associated clonal haematological non-mast cell lineage diseases: a histopathological challenge. *J Clin Pathol* 2004; **57**: 604–608.
13 Yang ZZ, Grote DM, Ziesmer SC, Manske MK, Witzig TE, Novak AJ *et al.* Soluble IL-2Ralpha facilitates IL-2-mediated immune responses and predicts reduced survival in follicular B-cell non-Hodgkin lymphoma. *Blood* 2011; **118**: 2809–2820.
14 Teodosio C, Garcia-Montero AC, Jara-Acevedo M, Alvarez-Twose I, Sanchez-Munoz L, Almeida J *et al.* An immature immunophenotype of bone marrow mast cells predicts for multilineage D816V KIT mutation in systemic mastocytosis. *Leukemia* 2012; **26**: 951–958.

Supplementary Information accompanies the paper on the Leukemia website (http://www.nature.com/leu)

Direct binding of Grb2 has an important role in the development of myeloproliferative disease induced by ETV6/FLT3

Leukemia (2013) **27,** 1433–1436; doi:10.1038/leu.2012.333

FMS-like tyrosine kinase 3 (*FLT3*) is one of the most frequently mutated genes in hematological malignancies.[1] The most common mutations of *FLT3* are internal tandem duplications (ITDs) within the juxtamembrane domain, which occur in 20% to 30% of patients with acute myeloid leukemia (AML).[2,3] Although FLT3 is a potential therapeutic target in AML, recent studies involving FLT3 inhibitors as single agents in patients with AML showed limited clinical responses.[4] FLT3 has been reported to fuse to ETV6 (TEL) in a few cases of myeloid/lymphoid neoplasms with eosinophilia (MLN-eo) carrying a translocation t(12;13)(p13;q12).[5,6] Although it has been shown that ETV6/FLT3 acts as a constitutively active tyrosine kinase, the molecular mechanisms underlying ETV6/FLT3-mediated leukemogenesis remain incompletely understood.[7–9]

We identified a novel *ETV6/FLT3* variant fusion transcript (E/F-1) in a MLN-eo patient (Supplementary Figures S1A and B) and investigated the transforming properties of ETV6/FLT3 *in vivo* using a murine bone marrow transplant (BMT) model.[10,11] E/F-1-transduced recipients developed an aggressive polyclonal myeloproliferative disease (MPD) in 100% of recipient mice with a latency of 3-4 weeks, as evidenced by marked leukocytosis, splenomegaly and massive expansion of myeloid cells in peripheral blood, spleen and bone marrow (Figures 1A–C). In this mice model, eosinophilia was not observed. Flow cytometric analysis of the peripheral blood from E/F-1 mice showed a large population of EGFP$^+$/Mac-1$^+$/Gr-1$^+$ cells. In primary E/F-1 mice, serial passage was performed by transferring a 1:1 mixture of spleen and bone marrow cells to sublethally irradiated recipient mice. This resulted in hematopoietic malignancies in most of the recipient mice receiving five different primary tumors. For three of the primary tumors, it was possible to transmit the MPD for at least one round. In all cases of serial passage, the MPD transformed into aggressive T-lymphoblastic lymphoma (T-LBL) with a latency of 4–17 weeks (Figure 1E, Supplementary Figure S2B). Most lymphoma occurred in the thymus or abdominal lymph nodes, and some of the secondary recipient mice displayed leukocytosis, generalized lymphadenopathy or hepatosplenomegaly. Histopathological examination revealed that the architecture of the lymph nodes and the thymus was completely effaced and that they contained a uniform population of lymphoblasts. The liver showed prominent periportal, lobular and sinusoidal

Accepted article preview online 20 November 2012; advance online publication, 14 December 2012

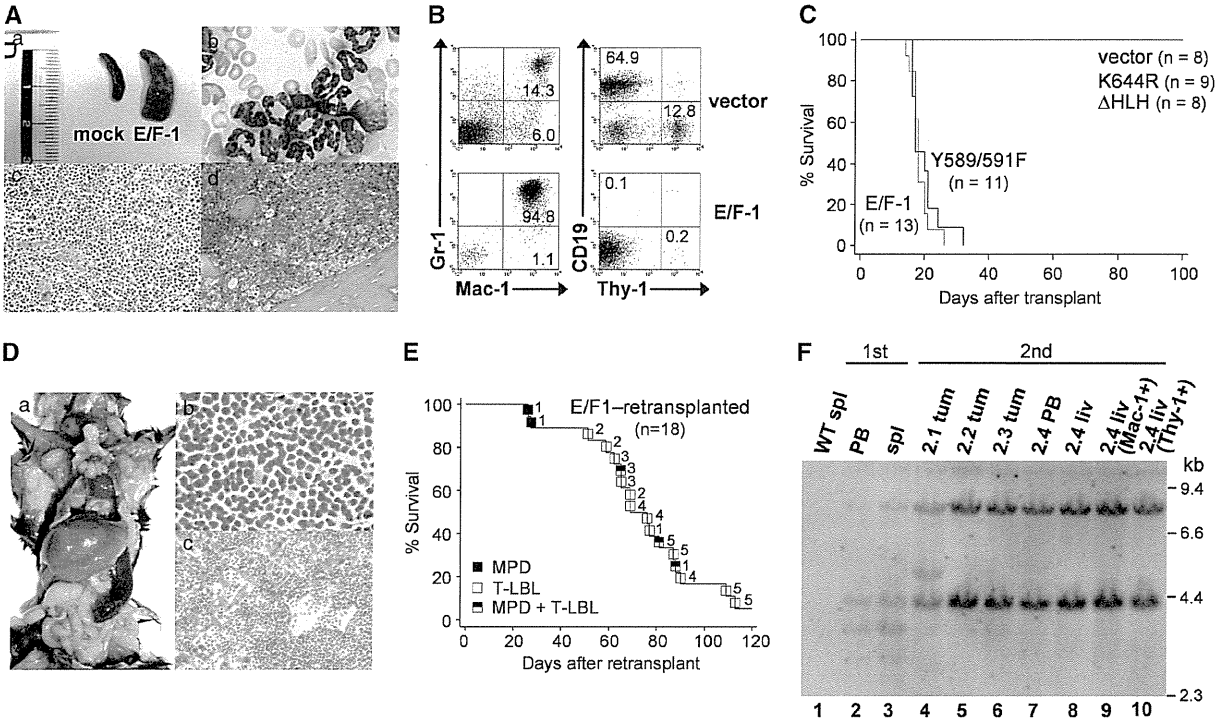

Figure 1. ETV6/FLT3 induces a rapidly fatal MPD in primary recipient mice, which transformed into T-LBL and MPD during serial passage. (**A**) (a) Splenomegaly associated with MPD. (b) Representative May–Giemsa-stained peripheral blood smear of the diseased mouse (× 100). (c, d) Representative hematoxylin and eosin-stained bone marrow (c) and spleen (d) of the diseased mouse (× 20). (**B**) Flow cytometric analysis of cells from the peripheral blood of vector control and E/F-1 mice. The percentages of cells in quadrants of interest are shown. (**C**) Survival curve for recipients of bone marrow transduced with a vector control ($n = 8$), E/F-1 ($n = 13$), Y589/591F mutant ($n = 11$), kinase-inactive K644R mutant ($n = 9$) or deletion mutant of the HLH oligomerization domain of ETV6 (ΔHLH) ($n = 8$). Mice transplanted with a vector control, K644R, or ΔHLH remain free of disease 180 days after transplant. Survival data are cumulative from two or three separate experiments for all retroviral constructs. (**D**) (a) Macroscopic examination of a secondary recipient with T-LBL (b and c) Hematoxylin and eosin-stained lymph node (b) and liver (c) of the diseased mouse (× 100 and × 20, respectively). (**E**) Kaplan–Meier survival analysis of the secondary recipients. Most secondary recipients succumbed to T-LBL or/and MPD. Pairs of recipients transplanted with cells from the same primary donor are indicated by numbers. (**F**) Proviral integrations in cells isolated from primary and secondary recipients. Genomic DNA isolated from the indicated tissues of a wild-type (WT) mouse (lane 1), a primary MPD mouse (lanes 2 and 3) and four secondary T-LBL mice receiving bone marrow and spleen from the same primary MPD mouse (lanes 4–10) was digested with *Eco*RI and analyzed for proviral integrations by hybridization with a DIG-labeled EGFP probe. Lanes 4–6 are DNAs from the tumors of mice with T-LBL. Lanes 7–10 represent lineage analysis from a single secondary mouse, which developed both MPD and T-LBL (2.4). The peripheral blood of the 2.4 mouse contained 83.5% EGFP$^+$Mac-1$^+$ and 10.6% EGFP$^+$Thy-1$^+$ cells, and the liver of the 2.4 mouse contained 27.2% EGFP$^+$Mac-1$^+$ and 58.8% EGFP$^+$Thy-1$^+$ cells at the time of euthanization. The MACS-sorted liver myeloid (Mac-1$^+$) and T cells (Thy-1$^+$) from this mouse were 98.1% and 98.4% pure, respectively. DNA size markers (in kb) are shown on the right. liv, liver; PB, peripheral blood; spl, spleen; tum, tumor.

infiltration by lymphoma cells (Figure 1D). Flow cytometric analysis of spleen cells revealed that the lymphomas typically showed an immature T-cell immunophenotype characterized by expression of both CD4 and CD8 (Supplementary Figure S2A). Affected tissues from secondary diseased mice contained proviral integrations identical to those in the primary MPD mouse (Figure 1F). ETV6/FLT3-induced T-LBL was transplantable, with all tertiary transplant recipients rapidly succumbing to T-LBL at 4–7 weeks after transfer arising from common clones identified in the secondary mice (Supplementary Figure S2C).

Previous studies have shown that FLT3-ITDs induce a lethal MPD in mice and that tyrosine residues 589 and 591 in the juxtamembrane domain of FLT3 are critical for STAT5 phosphorylation and generation of the MPD phenotype.[10] We also demonstrated the corresponding results for FLT3-ITD in our murine BMT experiment (Supplementary Figures S3A and B). On the other hand, mice that received the double tyrosine-to-phenylalanine mutant of E/F-1 at sites 589 and 591 (Y589/591F) in the juxtamembrane domain of FLT3 developed a similar MPD (Supplementary Table S1). There was no significant difference in survival between recipients of E/F-1 vs Y589/591F, with both mice groups succumbing to a fatal MPD within a median survival time of 18 and 19.5 days, respectively ($P = 0.284$; Figure 1C). The Y589/591F mutation did not abrogate STAT5, Erk1/2 and Akt activation in Ba/F3 cells transformed by E/F-1 (Supplementary Figure S4), which is consistent with the previous studies using a deletion mutant of the FLT3 juxtamembrane domain in ETV6/FLT3.[9]

Growth factor receptor-binding protein 2 (Grb2) is an adaptor protein known to bind several receptor tyrosine kinases. Grb2 binds the scaffolding protein Grb2-associated binder 2 (Gab2) and contributes to survival signaling in ligand-activated wild-type FLT3.[12] A recent study has shown that tyrosines 768, 955 and 969 of FLT3 are the direct Grb2-binding sites of importance for FLT3-ITD-mediated proliferation and survival of hematopoietic cells *in vitro* as a result of STAT5 activation via Gab2.[13] However, there have been no reports regarding the *in vivo* effects of direct Grb2 binding by oncogenic FLT3 in leukemogenesis. Thus, we investigated the role of Grb2 binding in ETV6/FLT3-mediated leukemogenesis. Inspection of the ETV6 portion of the fusion protein revealed only two candidate tyrosines for direct binding of

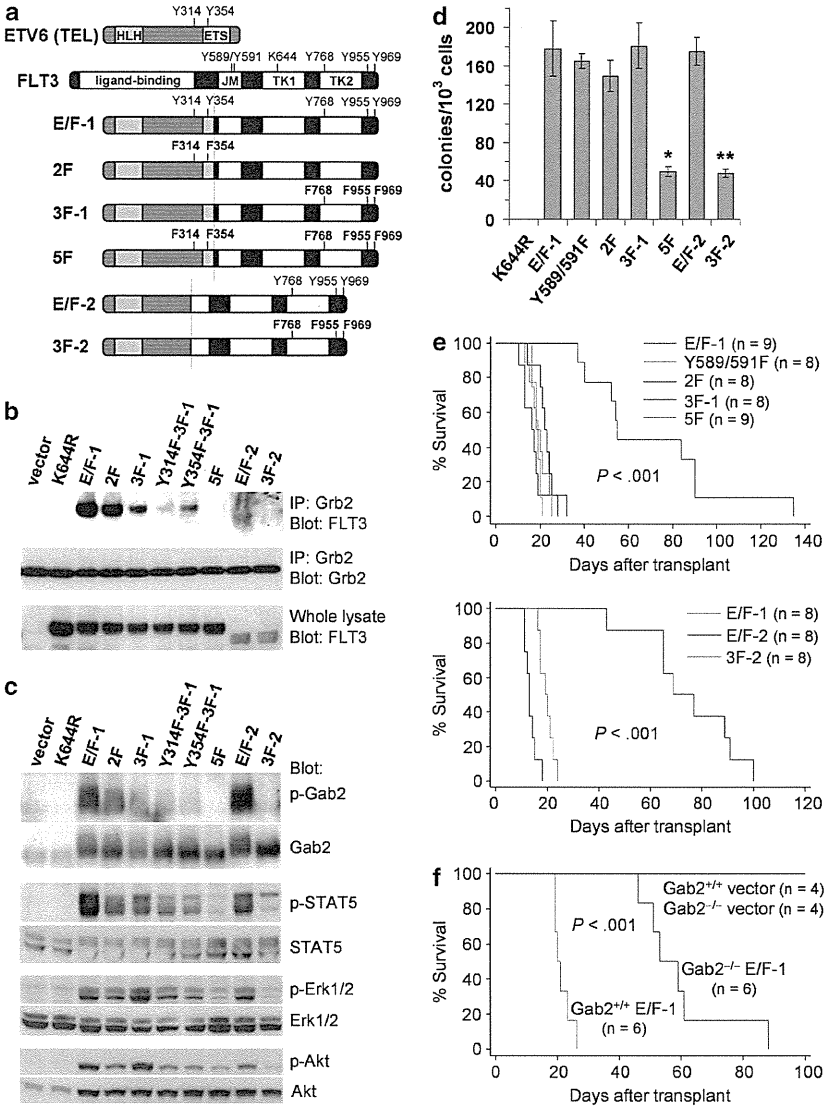

Figure 2. Both ETV6 and FLT3 portions contribute to ETV6/FLT3-mediated leukemogenesis via Grb2-Gab2 pathway. (**a**) Schematic representation of ETV6/FLT3 fusion proteins including the series of Grb2-binding site mutants. The point of fusion is indicated by a vertical dotted line. E/F-1 was cloned by us. E/F-2 was cloned previously (Vu *et al.*[5]). (**b**) Coimmunoprecipitation: lysates from Ba/F3 cells expressing the indicated ETV6/FLT3 proteins were immunoprecipitated using an anti-Grb2 antibody and blotted with anti-FLT3 (top) and anti-Grb2 (middle) antibodies. Whole-cell lysates were also blotted with the anti-FLT3 antibody (bottom). As a control, lysates from vector-transduced cells were included. Three independent experiments were performed and representative data are shown. (**c**) Activation of downstream targets was demonstrated by blotting the whole-cell lysates of Ba/F3 cells with the indicated phosphospecific antibodies. After stripping, the membranes were reprobed with the indicated total antibodies. Three independent experiments were performed and representative data are shown. (**d**) Cytokine-independent colony formation of whole bone marrow cells expressing ETV6/FLT3 wild-type or Grb2-binding mutants. The difference between E/F-1 and 5F (*) and between E/F-2 and 3F-2 (**) is statistically significant ($P<0.001$, unpaired *t*-test). Data are the mean ± s.d. of three independent experiments. (**e**) Survival curve for recipients of bone marrow transduced with ETV6/FLT3 and Grb2-binding mutants. Both E/F-1 and E/F-2 mice caused rapidly fatal MPD. 5F mutant mice and 3F-2 mutant mice developed MPD with a longer median survival of 55 and 73 days, respectively ($P<0.001$ vs E/F-1 and E/F-2, respectively). One of the 5F mutant mice died of severe anemia without showing any signs of MPD. Survival data are cumulative from two or three separate experiments for all retroviral constructs. (**f**) Survival curve for recipients of Gab2$^{-/-}$ and Gab2$^{+/+}$ bone marrow transduced with a vector control or E/F-1. The *P*-value represents a comparison of survival by E/F-1 on Gab2$^{-/-}$ vs Gab2$^{+/+}$ background.

Grb2 at positions 314 and 354. To test whether Grb2 binds directly to ETV6/FLT3, we made a series of Grb2-binding mutants of ETV6/FLT3 (Figure 2a). The Y314/354F double point mutant (2F) and the Y768/955/969F triple mutant (3F-1) of E/F-1 showed a reduced ability to bind Grb2 as compared with the E/F-1. Furthermore, when we mutated tyrosines 314 or 354 to phenylalanine in the context of the Y768/955/969F triple mutant, the association of ETV6/FLT3 with Grb2 was significantly reduced as compared with the Y768/955/969F triple mutant. Finally, when we mutated all five specific tyrosines (Y314/354/768/955/969) to phenylalanine, we observed that ETV6/FLT3 was no longer able to bind Grb2 (Figure 2b). Simultaneous mutation of these five tyrosine residues resulted in an absence of Gab2 phosphorylation, and impaired activation of STAT5, Erk1/2 and Akt in Ba/F3 cells (Figure 2c). ETV6/FLT3 variant E/F-2, which lacked the Grb2-binding sites of ETV6, was unable to bind to Grb2 when all three Grb2-binding sites of

FLT3 were mutated (Figure 2b). This Y768/955/969F triple mutant of E/F-2 (3F-2) was also unable to phosphorylate Gab2 and showed weaker activation of STAT5, Erk1/2 and Akt as compared with E/F-2 in Ba/F3 cells (Figure 2c). Both E/F-1 and E/F-2 transformed bone marrow cells to be capable of cytokine-independent growth in methylcellulose medium. Transformation was significantly decreased in the 5F and 3F-2 mutants, which were unable to bind Grb2, but not in 2F and 3F-1 mutants (Figure 2d). To examine the contribution of Grb2 binding to ETV6/FLT3-induced MPD *in vivo*, we performed BMT experiments. White blood cell (WBC) counts and spleen weights of the mice receiving 5F-transduced bone marrow were significantly lower than those receiving E/F-1-transduced bone marrow (Supplementary Table S1). Flow cytometric analyses of spleen cells showed that 5F mice had a reduced fraction of Mac-1^+/Gr-1^+ cells compared with E/F-1 mice (Supplementary Figure S5A). 5F mice showed significantly less infiltrate in the hepatic lobules or periportal areas than the E/F-1 mice (Supplementary Figure S5B). Recipients of both 2F and 3F-1 developed rapidly fatal MPD with a comparable latency to those of E/F-1. Survival of 5F and 3F-2 mice was significantly prolonged compared with that of E/F-1 and E/F-2 mice, respectively (55 days vs 18 days, 73 days vs 13 days, respectively; $P<0.001$; Figure 2e), although most 5F and 3F-2 recipient mice eventually succumbed to MPD.

Finally, we compared the ability of ETV6/FLT3 to transform primary myeloid cells from the bone marrow of Gab2$^{-/-}$ and Gab2$^{+/+}$ mice. Expression of E/F-1 in Gab2$^{-/-}$ cells resulted in an approximately threefold lower number of cytokine-independent CFU-C (Supplementary Figure S6A). We assessed the relative contribution of the *Gab2* gene to ETV6/FLT3-mediated leukemogenesis in BMT experiments using Gab2$^{-/-}$ and Gab2$^{+/+}$ donor mice. All mice transplanted with Gab2$^{+/+}$ bone marrow cells expressing ETV6/FLT3 developed severe MPD (median WBC, $236\times10^3/\mu l$; spleen weight, 561 mg), as expected (Supplementary Figure S6B). ETV6/FLT3-induced myeloproliferation was attenuated in mice transplanted with Gab2$^{-/-}$ bone marrow cells expressing ETV6/FLT3 (median WBC, $31\times10^3/\mu l$; spleen weight, 350 mg). Survival of mice injected with Gab2$^{-/-}$ bone marrow cells expressing E/F-1 was significantly prolonged in comparison with those injected with Gab2$^{+/+}$ cells (56 days vs 21 days, $P<0.001$; Figure 2f), although all recipients of Gab2$^{-/-}$ background bone marrow cells eventually succumbed to MPD.

Our results suggest that ETV6/FLT3 has more potent oncogenic activity than FLT3-ITDs and can transform progenitor cells with the capacity to differentiate into myeloid and lymphoid progeny, supporting the contention that human *ETV6/FLT3*-positive MLN-eo is a stem cell disorder. Unlike FLT3-ITDs, mice that received the Y589/591F mutant of ETV6/FLT3 also developed a lethal MPD with a short latency. The reason for the discrepancy between ETV6/FLT3 and FLT3-ITDs is not clear. This may be due to altered structural conformation of ETV6/FLT3 relative to wild-type FLT3 or alternatively, it may be due to different subcellular localization of the fusion protein and FLT3-ITDs.[14,15] Recently it was reported that sunitinib and sorafenib, tyrosine kinase inhibitors with multiple targets including FLT3, had therapeutic efficacy in two patients with *ETV6/FLT3*-positive MLN-eo.[6] Unfortunately, similar to most of the patients with *FLT3-ITD*-positive AML, relapse and resistance occurred in both patients. Although clinical application of Grb2 inhibitors remains limited to just a phase I trial of a liposomal antisense for hematological malignancies, the results of the current study indicate therapeutic potential against Grb2 in patients with *ETV6/FLT3*-positive MLN-eo. In addition, previous studies have shown that the Grb2-Gab2 pathway also has an important role in FLT3-ITD-mediated cell proliferation and survival.[13,15] These findings suggest that inhibition of this pathway may be useful in the treatment of FLT3-associated leukemia.

CONFLICT OF INTEREST

The authors declare no conflict of interest.

ACKNOWLEDGEMENTS

This work was supported in part by grants from the Ministry of Education, Culture, Sports, Science and Technology of Japan (MH).

K Chonabayashi[1], M Hishizawa[1], S Kawamata[2], Y Nagai[1], T Ohno[3], T Ishikawa[1], T Uchiyama[1] and A Takaori-Kondo[1]
[1]*Department of Hematology and Oncology, Graduate School of Medicine, Kyoto University, Kyoto, Japan;*
[2]*Foundation for Biomedical Research and Innovation, Kobe, Japan and*
[3]*Division of Hematology and Immunology, Department of Internal Medicine, Ohtsu Red Cross Hospital, Ohtsu, Japan*
E-mail: hishiza@kuhp.kyoto-u.ac.jp

REFERENCES

1 Stirewalt DL, Radich JP. The role of FLT3 in haematopoietic malignancies. *Nat Rev Cancer* 2003; **3**: 650–665.
2 Kiyoi H, Naoe T, Nakano Y, Yokota S, Minami S, Miyawaki S *et al.* Prognostic implication of FLT3 and N-RAS gene mutations in acute myeloid leukemia. *Blood* 1999; **93**: 3074–3080.
3 Thiede C, Steudel C, Mohr B, Schaich M, Schakel U, Platzbecker U *et al.* Analysis of FLT3-activating mutations in 979 patients with acute myelogenous leukemia: association with FAB subtypes and identification of subgroups with poor prognosis. *Blood* 2002; **99**: 4326–4335.
4 Kindler T, Lipka DB, Fischer T. FLT3 as a therapeutic target in AML: still challenging after all these years. *Blood* 2010; **116**: 5089–5102.
5 Vu HA, Xinh PT, Masuda M, Motoji T, Toyoda A, Sakaki Y *et al.* FLT3 is fused to ETV6 in a myeloproliferative disorder with hypereosinophilia and a t(12;13)(p13;q12) translocation. *Leukemia* 2006; **20**: 1414–1421.
6 Walz C, Erben P, Ritter M, Bloor A, Metzgeroth G, Telford N *et al.* Response of ETV6-FLT3-positive myeloid/lymphoid neoplasm with eosinophilia to inhibitors of FMS-like tyrosine kinase 3. *Blood* 2011; **118**: 2239–2242.
7 Tse KF, Mukherjee G, Small D. Constitutive activation of FLT3 stimulates multiple intracellular signal transducers and results in transformation. *Leukemia* 2000; **14**: 1766–1776.
8 Baldwin BR, Li L, Tse KF, Small S, Collector M, Whartenby KA *et al.* Transgenic mice expressing Tel-FLT3, a constitutively activated form of FLT3, develop myeloproliferative disease. *Leukemia* 2007; **21**: 764–771.
9 Vu HA, Xinh PT, Kano Y, Tokunaga K, Sato Y. The juxtamembrane domain in ETV6/FLT3 is critical for PIM-1 up-regulation and cell proliferation. *Biochem Biophys Res Commun* 2009; **383**: 308–313.
10 Rocnik JL, Okabe R, Yu JC, Lee BH, Giese N, Schenkein DP *et al.* Roles of tyrosine 589 and 591 in STAT5 activation and transformation mediated by FLT3-ITD. *Blood* 2006; **108**: 1339–1345.
11 Tanaka Y, Era T, Nishikawa S, Kawamata S. Forced expression of Nanog in hematopoietic stem cells results in a gammadeltaT-cell disorder. *Blood* 2007; **110**: 107–115.
12 Zhang S, Broxmeyer HE. Flt3 ligand induces tyrosine phosphorylation of gab1 and gab2 and their association with shp-2, grb2, and PI3 kinase. *Biochem Biophys Res Commun* 2000; **277**: 195–199.
13 Masson K, Liu T, Khan R, Sun J, Ronnstrand L. A role of Gab2 association in Flt3 ITD mediated Stat5 phosphorylation and cell survival. *Br J Haematol* 2009; **146**: 193–202.
14 Schmidt-Arras DE, Bohmer A, Markova B, Choudhary C, Serve H, Bohmer FD. Tyrosine phosphorylation regulates maturation of receptor tyrosine kinases. *Mol Cell Biol* 2005; **25**: 3690–3703.
15 Choudhary C, Olsen JV, Brandts C, Cox J, Reddy PN, Bohmer FD *et al.* Mislocalized activation of oncogenic RTKs switches downstream signaling outcomes. *Mol Cell* 2009; **36**: 326–339.

Supplementary Information accompanies this paper on the Leukemia website (http://www.nature.com/leu)

OPEN ACCESS Freely available online

PLOS ONE

Robust and Highly-Efficient Differentiation of Functional Monocytic Cells from Human Pluripotent Stem Cells under Serum- and Feeder Cell-Free Conditions

Masakatsu D. Yanagimachi[1,4], Akira Niwa[1], Takayuki Tanaka[1], Fumiko Honda-Ozaki[1], Seiko Nishimoto[1], Yuuki Murata[3], Takahiro Yasumi[3], Jun Ito[1], Shota Tomida[1], Koichi Oshima[1], Isao Asaka[2], Hiroaki Goto[4], Toshio Heike[3], Tatsutoshi Nakahata[1], Megumu K. Saito[1]*

1 Department of Clinilcal Application, Center for iPS Cell Research and Application, Kyoto University, Kyoto, Japan, **2** Department of Fundamental Cell Technology, Center for iPS Cell Research and Application, Kyoto University, Kyoto, Japan, **3** Department of Pediatrics, Kyoto University Graduate School of Medicine, Kyoto, Japan, **4** Department of Pediatrics, Yokohama City University Graduate School of Medicine, Yokohama, Japan

Abstract

Monocytic lineage cells (monocytes, macrophages and dendritic cells) play important roles in immune responses and are involved in various pathological conditions. The development of monocytic cells from human embryonic stem cells (ESCs) and induced pluripotent stem cells (iPSCs) is of particular interest because it provides an unlimited cell source for clinical application and basic research on disease pathology. Although the methods for monocytic cell differentiation from ESCs/iPSCs using embryonic body or feeder co-culture systems have already been established, these methods depend on the use of xenogeneic materials and, therefore, have a relatively poor-reproducibility. Here, we established a robust and highly-efficient method to differentiate functional monocytic cells from ESCs/iPSCs under serum- and feeder cell-free conditions. This method produced $1.3\times10^6\pm0.3\times10^6$ floating monocytes from approximately 30 clusters of ESCs/iPSCs 5–6 times per course of differentiation. Such monocytes could be differentiated into functional macrophages and dendritic cells. This method should be useful for regenerative medicine, disease-specific iPSC studies and drug discovery.

Citation: Yanagimachi MD, Niwa A, Tanaka T, Honda-Ozaki F, Nishimoto S, et al. (2013) Robust and Highly-Efficient Differentiation of Functional Monocytic Cells from Human Pluripotent Stem Cells under Serum- and Feeder Cell-Free Conditions. PLoS ONE 8(4): e59243. doi:10.1371/journal.pone.0059243

Editor: Katriina Aalto-Setala, University of Tampere, Finland

Received August 14, 2012; **Accepted** February 13, 2013; **Published** April 3, 2013

Funding: Funding was provided by grants from the Ministry of Health, Labour and Welfare to TN, a grant from the Ministry of Education, Culture, Sports, Science and Technology (MEXT) to TN, grants from the Leading Project of MEXT to TN, a grant from Funding Program for World-Leading Innovative Research and Development on Science and Technology (FIRST Program) of Japan Society for the Promotion of Science (JSPS) to TN, grants from JSPS to TN and MKS, grants from the Takeda foundation, Mitsubishi Pharma Research Foundation and Suzuken memorial foundation to MKS and grants from Grants-in-Aid for Scientific Research from Japan Society for the Promotion of Science from the Ministry of Education, Culture, Sports, Science, and Technology of Japan to MDY. The funders had no role in study design, data collection and analysis, decision to publish, or preparation of the manuscript.

Competing Interests: The authors have declared that no competing interests exist.

* E-mail: msaito@cira.kyoto-u.ac.jp

Introduction

Monocytic lineage cells, such as monocytes, macrophages and dendritic cells (DCs), are central to immune responses and play key roles in various pathological conditions. [1–2] Monocytes are the myeloid progeny of hematopoietic stem/progenitor cells [3]; they are a type of mononuclear cell circulating in the bloodstream and act as gatekeepers in innate immunity. While they replenish macrophages and DCs, monocytes themselves respond to various inflammatory stimuli by migrating into inflamed tissues, phagocytosing pathological small particles and producing proinflammatory cytokines and chemokines. Therefore, monocytes not only contribute to host defense against pathogenic microorganisms, but are closely associated with the pathogenesis of chronic sterile inflammation. [4] Macrophages reside in tissues and robustly phagocytose microorganisms and cellular debris. One of the important hallmarks of monocytic lineage cells is their functional plasticity. In response to cytokines and microbial products, macrophages polarize into functionally distinct M1 and M2 cells. [5] Classically activated M1 macrophages are induced by interferon-γ (IFNγ), while alternatively activated M2 macrophages can be induced by IL-4 and IL-13. [2,5] M1 macrophages are generally characterized by high production of proinflammatory cytokines, while M2 are characterized by high production of anti-inflammatory cytokines. DCs are the most powerful antigen-presenting cells and have an indispensable role for the activation of T lymphocytes. Because of their ability to mediate communication between innate and acquired immunity, ex vivo expansion of DCs is expected to be a useful source of material for cancer immunotherapies, such as DC-based vaccines. [6–7] Moreover, recent reports of monocyte and/or DC deficiencies highlight the importance of understanding their development in humans. [8] However, there have been technical limitations for tracing the development of human monocytic cells, or for propagating them ex vivo.

Human embryonic stem cells (ESCs) and induced pluripotent stem cells (iPSCs) are undifferentiated pluripotent cells that can be propagated indefinitely. [9–11] The development of monocytic cells from these pluripotent cells is of particular interest because it would provide an unlimited source of these cells for clinical applications and the examination of disease pathologies. Although the methods for hematopoietic differentiation from ESCs/iPSCs

using embryonic body or feeder co-culture systems have already been established, [12] these methods usually depend on xenogeneic feeder cells and/or animal- or human-derived serum, and therefore have a relatively poor-reproducibility. For instance, batch-to-batch variability of serum or feeder cells can influence the characteristics of *in vitro* differentiated DCs. [13] Here, we describe a novel serum- and feeder cell-free method that robustly and repetitively produces monocytic lineage cells from human ESCs/iPSCs.

Materials and Methods

Cell Culture

This study used human ESCs (cell line: KhES1) and iPSCs (cell lines: 201B7, 253G4, CIRA188Ai-W2, and CB-A11). [10,14–15] 201B7, 253G4 [10] and CIRA188Ai-W2 [15] were previously described. A human ES cell line KhES1 was kindly provided by Dr. Norio Nakatsuji. Human iPS cell lines 201B7 and 253G4 were kindly provided by Dr. Shinya Yamanaka. CB-A11 was established from cord-blood mononuclear cells by using episomal vectors. [16] These ESCs/iPSCs were maintained on tissue culture dishes coated with growth factor-reduced Matrigel (Becton-Dickinson) in mTeSR1 serum-free medium (STEMCELL Technologies).

Monocytic Lineage Cell Differentiation Method

The monocytic lineage differentiation protocol was modified from a previously established hematopoietic differentiation protocol (Figure 1). [17] The protocol consists of 5 sequential steps by which mature MPs and DCs are differentiated from human pluripotent cells in a stepwise manner. In the first step, primitive streak cells were induced from undifferentiated ESCs/iPSCs, which were then differentiated into hemangioblast-like hematopoietic progenitors in the second step. In step 3, expanded hematopoietic progenitors were committed towards initial myeloid differentiation, and then differentiated into the monocytic lineage in step 4. Finally, $CD14^+$ monocytes were differentiated into either MPs or DCs in step 5. The cytokines used in this study were purchased from R&D systems.

Step 1: induction of primitive streak-like cells from undifferentiated human ES/iPS cells with BMP4. BMP4 is an important molecule for the initial stage of mesodermal commitment of pluripotent stem cells in vitro. [17] Undifferentiated ESCs/iPSCs colonies were disseminated onto a 100 mm culture dish coated with growth factor-reduced Matrigel in mTeSR1 medium at a density of about 30 colonies per dish. Individual colonies were grown to a diameter of approximately 1 mm (Day 0), and BMP4 (80 ng/mL) was added to the mTeSR1 medium.

Step 2: generation of KDR^+CD34^+ hemangioblast-like cells with VEGF, basic FGF and SCF. VEGF and SCF have been reported to be important cytokines for development of hemoangiogenic progenitors. [18–19] In this step, we also added basic FGF which enhances the development of mesodermal hematopoietic progenitors. [18,20] The mTeSR1 medium was replaced by StemPro-34 serum-free medium (Gibco) containing 2 mM glutamax (Invitrogen) on day 4, and then was supplemented with the step-2 cytokine cocktail composed of VEGF (80 ng/mL), basic FGF (25 ng/ml), and SCF (100 ng/mL).

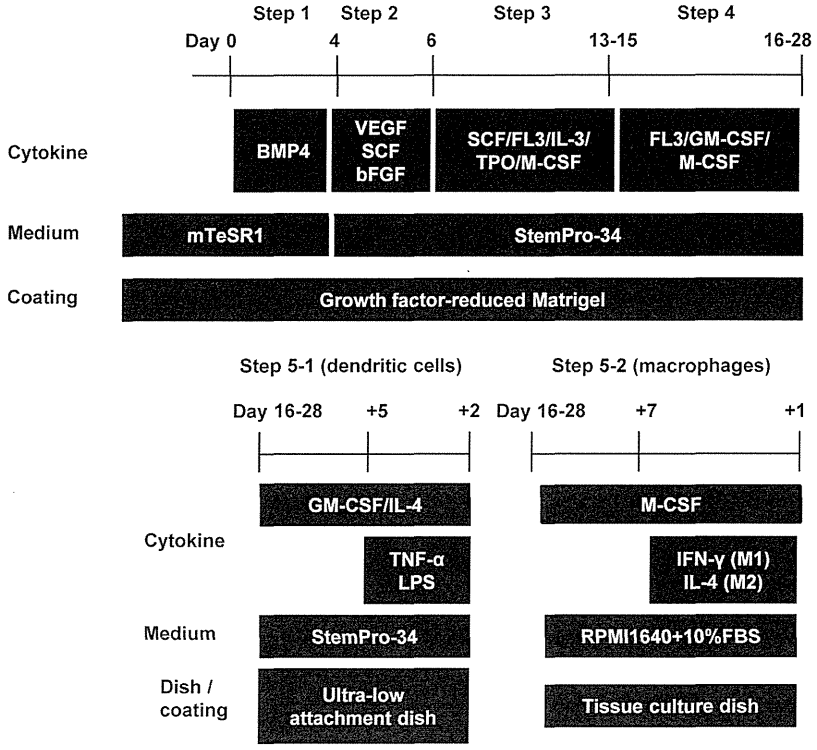

Figure 1. Protocol for monocytic lineage cell differentiation from human pluripotent stem cells. The protocol is composed of 5 steps. CD14-positive cells that are sorted between step-4 are differentiated into dendritic cells by step 5-1 or into macrophages by step 5-2. FL-3: Flt-3 ligand, TPO: Thrombopoietin.
doi:10.1371/journal.pone.0059243.g001